TABLE OF CONTENT

LIST OF FIGURES

LIST OF TABLE

Results of a Geophysical and Sedimentological Evaluation: Tiger-Trinity Shoal as Sources of Sand for Coastal Restoration

EXECUTIVE SUMMARY

This investigation was undertaken as a collaborative and cooperative effort between the Bureau of Ocean Energy Management, Regulation and Enforcement (BOEMRE, previously the Minerals Management Service, MMS), Louisiana Office of Coastal Protection and Restoration (OCPR, previously the Louisiana Department of Natural Resources, LDNR) and the Coastal Studies Institute (CSI) at Louisiana State University (LSU). The Tiger-Trinity research activities were carried out under Cooperative Agreement No. M07AC12517 between MMS and LDNR (OCPR) and CSI at LSU. The Louisiana OCPR contracted CSI under Interagency Agreement No. 2512-07-12 to undertake the evaluation of sand resources in the Tiger-Trinity Shoals Complex for coastal restoration in Louisiana.

Comprehensive geophysical and sedimentological datasets including (a) high resolution subbottom profiles, (b) bathymetry, (c) magnetometer anomalies, (d) side-scan sonar swaths, and (e) vibracores were collected in order to evaluate sand resources within the human infrastructure of the Tiger-Trinity Shoals Complex. The geophysical data were acquired on a grid totally 750 line mi (1200 line km). In order to calibrate the stratigraphic framework established from the subbottom data, a total of 46 vibracores up to 13 ft. (4 m) long were collected throughout the Tiger-Trinity Shoals Complex. Magnetometer data acquired on the transects of the survey grid defined the oil and gas infrastructure of pipelines, production platforms, and isolated magnetic anomalies. These data partitioned the sand bodies of both shoals into polygonal areas where potential sand extraction could take place, considering a buffer zone of 1000 ft. (305 m) from pipelines as mandated by state and federal regulations. The total sand volume in Tiger Shoal was calculated to be 58.6 x 10^6 yd^3 (44.8 x 10^7 m^3) of the sands ranged in size from 0.0.768-0.123 mm. The total sand volume in Trinity Shoal was 893.2 x 10^6 yd^3 (687.7 x 10^6 m^3). Like Tiger Shoal, sands of Trinity Shoal were of very fine sand size (0.0625-0.125 m). It is important to note that the total volume of sand in the two shoals calculated from this study's data is less than half the volume calculated by Penland et al. (1990) in their 1980s study.

Because of oil and gas infrastructure, Trinity Shoal was partitioned into four polygonal areas and Tiger Shoal into one polygon from which sand could be potentially extracted. Considering these polygons the total volume of extractable sand in Trinity Shoal (four separate areas) was 432.9 x 10^6 yd^3 (330.9 x 10^6 m^3) and 19.6 x 10^6 yd^3 (15.0 x 10^6 m^3) for Tiger Shoal. Five isolated magnetic anomalies were identified within the areas defined for potential future sand extraction. These anomalies would have to be examined in detail before the polygonal areas in which they occur could be cleared for sand extraction.

In summary, the Tiger-Trinity Shoals represent a large source of sand that could be harvested for coastal restoration purposes. Although there is considerable oil and gas activity and associated infrastructure in the area, large areas of the two shoals remain acceptable for sand extraction. Barring new infrastructure development, the areas defined by this study contain large volumes of sand that can be utilized by the State of Louisiana for coastal reclaimation projects.

INTRODUCTION

The low-relief deltaic landscape of south Louisiana is extremely vulnerable to the combined effects of sea level rise, tropical storm impacts, and the many aspects of coastal plain subsidence. As a result of these and other conditions such as a diminishing supply of sediment to the Mississippi River, (Blum and Roberts, 2009) landloss in coastal Louisiana is the highest in the nation. Since the 1930s Louisiana has lost 1829 mi^2 (4737 km^2) of coastal wetlands (Britsch and Dunbar, 1993; Barras et al., 2008). Field et al. (1991) and Dahl (2000) point out that Louisiana accounts for about 30% of the nation's coastal wetlands, and at the same time Louisiana also accounts for approximately 90% of the coastal marsh loss in the America's contiguous states. Barras et al. (2003) project that 500 mi^2 (1295 km^2) of coastal land will be lost over the next 50 years, even with current levels of coastal restoration. A more dramatic estimate of landloss has recently been presented by Blum and Roberts (2009). They calculate that because of a continued increase in eustatic sea level rise, persistent coastal plain subsidence, and a diminished sediment load for the Mississippi River a total of 3861-5212 mi^2 (10,000-13,500 km^2) of coastal plain land will be lost by the year 2100. This figure does not include significant and inevitable losses to Louisiana's sandy barrier islands.

The barrier islands along Louisiana's coast represent the wave and current reworked distal ends of former delta complexes that over the last ~ 7000-7500 years have collectively constructed the Louisiana coastal plain (Penland et al., 1988; Roberts, 1997). These sandy barriers derive their coarse sediment from the reworking of distributary mouth bar, channel, and crevasse-splay deposits that comprise important depositional elements of the deltaic landscape. At the same time, the fine-grained components of these depositional environments are transported away from the site of reworking, while the coarse fraction (fine sands and silts) is concentrated. Once formed, the resulting barrier islands and associated shoals function as physical buffers between open marine continental shelf processes and the bays and surrounding marshlands that occur inland of the barriers. Many coastal researchers and environmental managers recognize the importance of Louisiana's barriers as the state's first line of defense against destructive wave action that erodes the marshland perimeter and thereby adds to the general landloss of the coastal plain (Stone et al., 2005; Georgiou et al., 2005). Waves capable of eroding the marsh do not have to be generated by storms, but can be normal shelf- and bay-generated wind waves that constantly interface with the marsh perimeter (Stone et al., 2005). The barrier islands protect back-barrier and bay perimeter environments from direct impingement of shore-directed wind waves generated on the continental shelf.

Hurricanes, tropical storms, and extra tropical storms, however, have the potential of doing enormous damage to Louisiana's barrier islands and back-barrier marshlands. For example, the United States Geological Survey (USGS, Barras et al., 2008) estimated that over 203 mi^2 (~ 526 km^2) of marshland was converted to open water as a product of the combined effects of Hurricanes Katrina and Rita. Elevated water levels and aggressive wave action associated with large storms can breach barrier islands and redistribute sediments over long stretches of the Louisiana coast. Much of this redistributed coarse sediment is nonrenewable to the barrier system and therefore is lost as part of the "coastal defense network." Because the northern Gulf of Mexico is a frequent corridor for hurricanes (Keim et al., 2007), Louisiana barriers are constantly stressed by hurricane-forced waves and currents. The net result when

combined with subsidence is that the sediment source-limited barriers along the Louisiana coast are constantly being degraded with no available natural process of restoring themselves even during periods of constructive wave-current activity. These interactions indicate that storms put Louisiana's barrier islands in a setting that always results in a net loss of sediment to the system. Therefore, in order to maintain the barriers as a buffer to our marshlands against both normal long-fetch wind waves and the effects of storms, coastal scientists have advocated the rebuilding of Louisiana barriers and their dunes by adding sediment, especially sands to the barrier island systems. This activity as well as rebuilding beaches that front coastal marshlands requires a sand resource available for restoration projects that is in the vicinity of the proposed project area and can be cost-effective to extract and transport to the project site.

PURPOSE OF THE TIGER-TRINITY SHOAL STUDY

Within the river-dominated deltaic setting of the Louisiana coastal plain and associated inner shelf, sands and coarse silts suitable for barrier and beach restoration are concentrated in only a few primary depositional settings such as channels, distributary mouth bars, and crevasse-splays or subdeltas (Finkl and Khalil, 2005; Finkl et al., 2006). By far, most of the coastal plain is dominated by fine-grained sediments. Therefore, locating sand resources of adequate size, sediment quality, and in a location feasible to extract for restoration purposes is a challenge. The sedimentary architecture of Louisiana's delta complexes that built the coastal plain is one that is characterized by both high rates of lateral and vertical variability in sedimentary facies. This highly variable sedimentary framework makes exploration for adequate restoration sand resources a problem that requires data collection strategies that incorporate high resolution subbottom information collected in dense survey grids (Khalil, 2004, 2008).

Distributary networks, their prograded mouth bars, channel-associated levees, and crevasse splays can be traced through Louisiana's bays onto the inner continental shelf. From Atchafalaya Bay to Chandeleur Sound these channels and their associated depositional units are related to various episodes of delta-building that started with the Maringouin-Sale Cypremort Complex of west-central Louisiana over 7000 years ago. Although paleo-channels of Pleistocene age are proven sand resources on the inner shelf along the western Louisiana coast where depositional rates in the Holocene have been comparatively low, channels of similar age are generally covered with too much overburden to be considered sand resources for restoration along the central and eastern Louisiana coasts. Even though these channels have been observed in the shallow subsurface along the western Louisiana coast, they are sparsely distributed, and many are covered with too much overburden to make them economically feasible as sources of sand for coastal restoration. Therefore, the most feasible sand resource for the west-central Louisiana coast would be the Tiger-Trinity Shoals Complex seaward of Marsh Island and Vermillion, West Cote Blanche, and East Cote Blanche Bays. These shoals are approximately 25 mi (40 km) from Chenier Au Tigre and Marsh Island, near areas where coastal restoration projects are being considered.

A previous study of Tiger-Trinity Shoals by the Louisiana Geological Survey (Penland et al., 1989; Suter et al., 1991) identified them as enormous potential resources of offshore sand, but sufficient details about the shoals were missing from this work to warrant resurveying to make sure adequate sand resources are available for extraction within the matrix of oil and gas

infrastructure in the area. Figure 1 shows the location of these shoals in the context of the central Louisiana coast. This second and more detailed investigation of the shoals was undertaken by the Louisiana Office of Coastal Protection and Restoration (OPCR) and the Coastal Studies Institute at Louisiana State University with funding from the Minerals Management Service (MMS) which has recently been renamed the Bureau of Ocean Energy Management, Regulation and Enforcement (BOEMRE). Primary objectives of this investigation were: (1) evaluate the quantity and quality of sand in the Tiger-Trinity Shoals Complex using high resolution subbottom profiling and vibracoring, (2) from magnetometer data, determine the location of pipelines and other metallic obstructions to a potential sand-mining operation, and (3) calculate both the total volume of sand in the shoals and sand available for extraction considering the current infrastructure constraints and identify the most probable sand-mining areas.

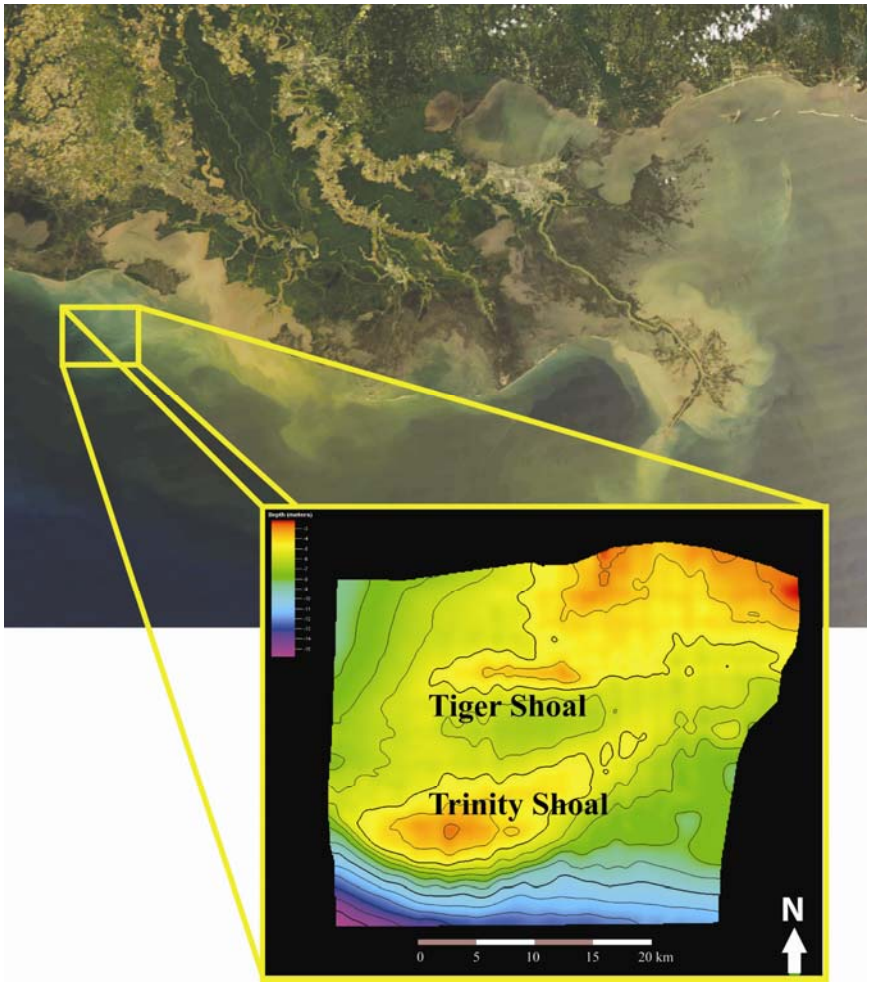

Figure 1. Location map showing the relation of Tiger and Trinity Shoals to the central Louisiana coast.

PRESENT UNDERSTANDING OF HOLOCENE GEOLOGIC FRAMEWORK

During the last glacial period, sea level lowered as ice sheets expanded across the continents. By the end of the last glacial maximum (ca. 21 ka), eustatic sea level was at the shelf margin, 395 ft. (~120 m) below present (Peltier and Fairbanks, 2006). This drop in base level, coupled with intermittent glacial outwash, induced fluvial entrenchment of the Lower Mississippi Valley (Fisk, 1944; Fisk and McFarlan, 1955; Autin et al., 1991; Saucier, 1994). Upon deglaciation, eustatic sea-level rise incrementally inundated the northern Gulf of Mexico's continental shelf, eventually flooding the Mississippi River's Pleistocene alluvial valley (Fisk and McClelland, 1959). These two post-glacial parameters, rising eustatic sea level and the incised Mississippi River valley, fundamentally influenced the timing of Holocene Mississippi River Delta Plain evolution: it was not until ca. 8 ka, after the deceleration of eustatic sea-level rise and the sediment infilling of the incised valley, that the Mississippi River's first delta complex, the Maringouin, prograded out onto the continental shelf (Frazier, 1967).

Delta building is an inherently cyclical process, consisting of a fluvial-dominated regressive phase and a marine-dominated transgressive phase (Fisk, 1944; Fisk and McFarlan, 1955; Kolb and Van Lopik, 1958). During the regressive phase, a sufficient quantity of sediment is supplied to the receiving basin via the main channel and its distributaries, such that sediment deposition overwhelms the ability of marine processes to remove that sediment (Scruton, 1960). Consequently, the delta shoreline advances seaward as sediment infills the available accommodation. As a delta continues to prograde, the fluvial system eventually becomes overextended, and therefore unstable. Up-stream avulsion will follow as the river seeks a more direct, hydraulically efficient route to the sea. This process of stream abandonment, which is responsible for the spatial shift of individual deltaic depocenters, is termed "delta switching" (Fisk, 1944; Fisk and McFarlan, 1955; Kolb and Van Lopik, 1958).

Delta switching occurs on a variety of temporal and spatial scales, producing a conglomeration of deltaic depositional features that offset and overlap on a variety of temporal and spatial scales, hence the phrase "deltas within deltas" (Roberts, 1997). At the top of the Mississippi River Delta hierarchy, in both a spatial and temporal sense, is the all-encompassing delta plain. Within the delta plain are delta complexes, sedimentary sequences that are each associated with a single major channel of the Mississippi River. Figure 2 shows the six major delta complexes, in geochronologic order, that comprise the Holocene delta plain. Within each delta complex are several individual delta lobes. Frazier (1967) identified a total of 16 delta lobes. Fourteen of these were determined within the Teche, St. Bernard, and Lafourche. Two delta lobes are attributed to the Plaquemines-Balize delta. None were identified within the Maringouin as radiocarbon age control was too sparse. Constituting delta lobes are sub-deltas and smaller crevasse splays, which build into shallow bays as secondary channels break through the natural levees of major distributaries (Coleman and Gagliano, 1964).

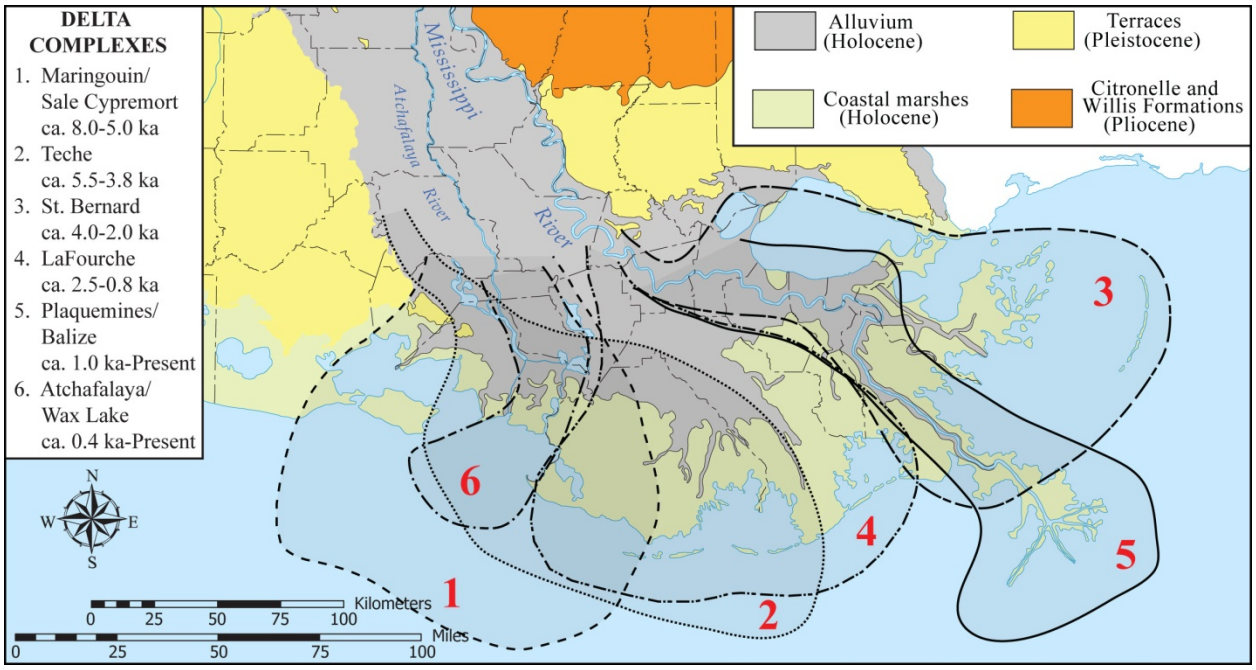

Figure 2. The Mississippi River Delta Plain. The six major delta complexes, with approximate ages and aerial extent, are indicated (modified from Roberts (1997)).

In addition to shifting the depocenter to a new location within the delta plain, up-dip avulsion initiates the transgressive phase of the older delta, though not necessarily immediately. Both channels, new and old, share the flow and sediment load initially, but as the new course begins capturing a greater percentage of the total, the previously active delta begins to yield to subsidence-driven and marine-reworking processes (Roberts, 1997). The transgressive evolution of a delta is first perceived by an erosional headland (Fig. 3), as waves and long-shore currents rework the distributary mouth-bar sands laterally to form characteristic flanking spits and barriers (Penland and Boyd, 1981; Penland et al., 1985; 1988). Behind the barrier system, semi-enclosed interdistributary bays open up and expand as subsiding back-barrier marshes submerge (Stage 1 of the Penland and Boyd (1981) model). Subsidence is relentless, leading to further degradation of back-barrier marshes, complete submergence of the erosional headland, and the coalescing of interdistributary bays into a back-barrier lagoon. Detached from the mainland, the transgressive sand bodies form a barrier island arc (Stage 2). As the barrier islands progressively migrate landward, in the course of time they become removed from their sediment source, i.e. the channel sands and distributary mouth bar deposits that were deposited basinward within the now underlying delta. This relationship has significant implications in regards to reoccurrence of hurricanes and the associated barrier island destruction they cause. With no new sediment introduced to the system, barrier islands reemerge post-storm with a net loss of sediment. Subsidence and marine reworking processes continue unabated, ultimately overcoming the diminished barrier island's ability to remain subaerial. Transgression culminates with the transformation of the barrier island arc into a submarine shoal (Stage 3).

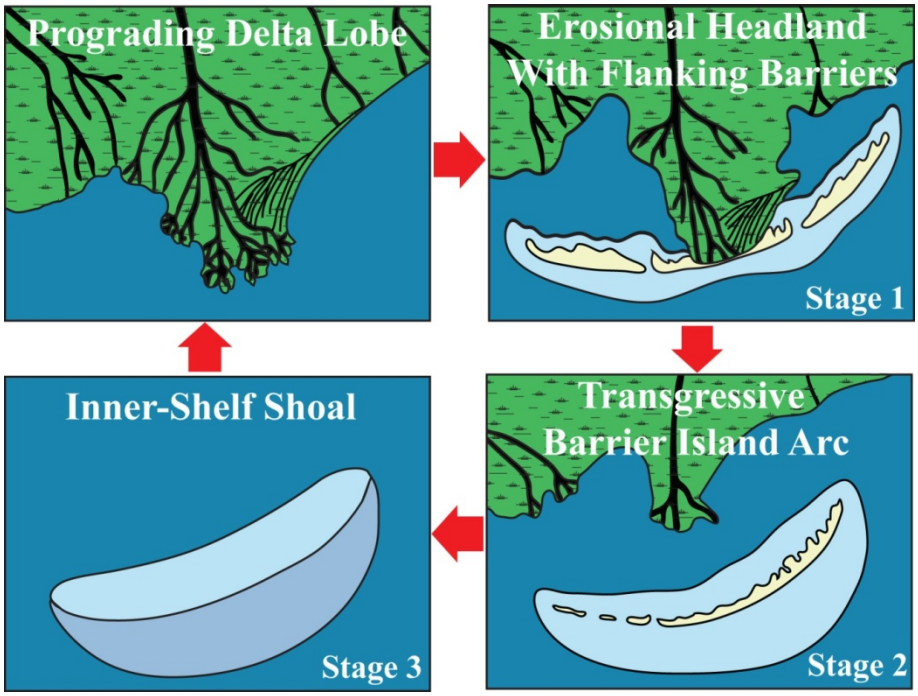

Figure 3. The evolution of a transgressing delta lobe, depicted graphically as a 3 stage process. Transgression begins with Stage 1, an erosional headland with flanking spits and barriers. In Stage 2, the barrier island arc detaches from the mainland. Ultimately, barrier islands succumb to subsidence and reworking processes, and form a submarine sand shoal in Stage 3 (modified from Penland et al., 1988).

Figure 4 displays all components, regressive and transgressive, of the delta cycle. Trinity and Tiger Shoals, the study area of this report, represent its cessation. Trinity and Tiger Shoals are shore parallel-to-concave-landward submarine sand bodies positioned 18.5 – 25 mi (~30-40 km) offshore of west-central Louisiana. Trinty Shoal stretches almost 18.5 mi (50 km) in length, extends as much as 6 mi (10 km) in width (not including the relatively thin sand sheet that protrudes an additional 5 mi (~ 8 km) off its northwestern perimeter), and reaches a thickness of 23+ ft (7+ m) in some areas. The much smaller Tiger Shoal stretches 7.75 mi (12.5 km) in length, extends its width more the 2.5 mi (4 km) in some areas, and has a maximum thickness of 6.75 ft (2+ m). The mean sand fraction of Trinity Shoal appears to be entirely very-fine sand, whereas Tiger Shoal's mean sand fraction ranges from medium sand (in its extreme eastern section) to very-fine sand. Trinity and Tiger Shoals are separated by approximately > 6 mi (> 10 km) of muddy-to-clay sediment in the east, whereas a thin recurved sand body coming off the north-west portion of Trinity Shoal appears to weld to Tiger Shoal in the west. Some confusion does exist in the literature in regards to their origin (Frazier, 1967; Penland et al., 1988). Is Trinity Shoal genetically linked to the Maringouin Delta Complex, or are both shoals of Teche origin? If Trinity Shoal is of Maringouin origin, then a still-rising eustatic sea level of this time period (ca. 8,000-6,000 ka), in addition to subsidence, would have considerably accelerated the transgressive phase described above, and perhaps led to more of an "in-place drowning" of the paleo-Trinity barrier island arc.

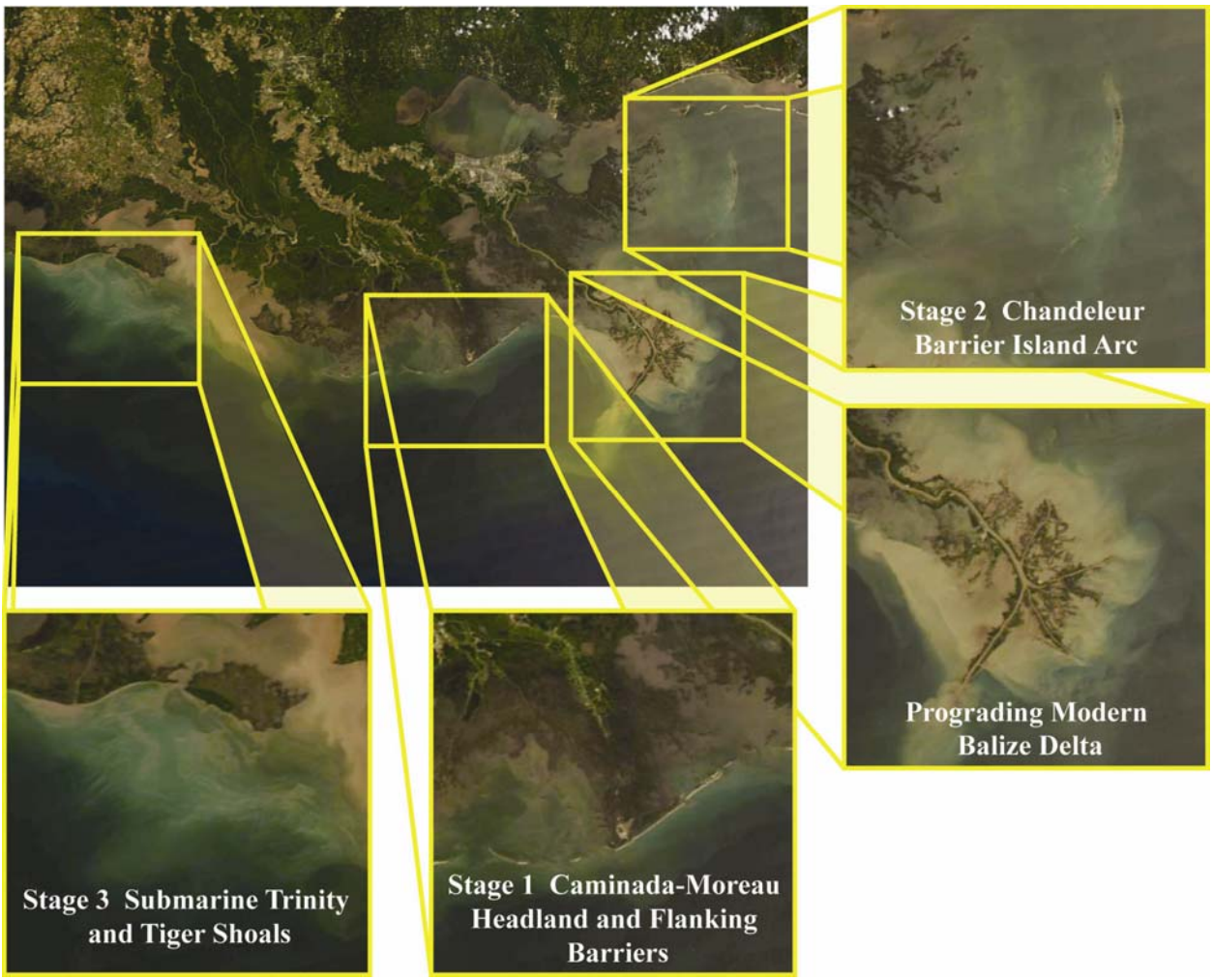

Figure 4. The present Mississippi River Delta Plain displays all depositional components, regressive and transgressive, of the delta cycle. The modern Balize delta represents the regressive phase of the delta cycle. The Lafourche Delta is in Stage 1 of the transgressive phase, with its eroding headland providing sediment for downdrift barrier growth. The St. Bernard Delta long ago entered Stage 2 of transgression, leaving the Chandeleur Islands stranded in open water. Trinity and Tiger Shoals represent the final phase, Stage 3 of transgression. Though yet determined, these shoals have previously been suggested to be remnants of both the Maringouin and Teche delta complexes. MODIS (Moderate Resolution Imaging Spectroradiometer) Satellite image of the Mississippi River Delta Plain, taken from the Louisiana State University Earth Scan Laboratory (www.esl.lsu.edu).

RATIONALE OF APPROACH AND METHOLOGIES

The previous work on Tiger-Trinity Shoals accomplished by the Louisiana Geological Survey and the United States Geological Survey in the 1980s proved that these transgressive sediment bodies contain large volumes of sand that have the potential to be used for coastal restoration purposes (Penland et al., 1989, Suter et al., 1991). The high resolution seismic data

on which these researchers based their appraisals of sand body geometry were analog ORE Geopulse "boomer" records of marginal quality. However, these records were calibrated to 30 excellent vibracores, some over 40 ft. (12 m) in length. Each vibracore was described and observations recorded in graphic log format. Their survey covered 500 line miles (800 line km) with a line spacing of approximately 3 mi (5 km). Navigation for seismic acquisition and vibracore sites was provided by LORAN.

A significant shift in technology, the analog-to-digital transition, occurred after the initial Tiger-Trinity survey described above. Data collection associated with the present investigation of Tiger-Trinity Shoals described in this report incorporated the most up-to-date digital acquisition and data management systems. In addition, all data sets were spatially located with satellite-corrected GPS technology which provided submeter accuracy. The rational for conducting the latest investigation of Tiger-Trinity Shoals was to focus the most recent data collection technology on a less regional appraisal of sand resources in this system than the 1980's survey. At the same time, this new investigation considers the oil and gas infrastructure that has expanded in the area since the 1980s and partitions the sand bodies and their feasibility as potential sand extraction sites. Toward these ends, over 750 line miles (1200 line km) of high resolution subbottom, bathymetry, and side-scan sonar data were collected along with 46 vibracores during the 2007-2008 field seasons (Figure 5). The methodologies employed in data collection are explained below.

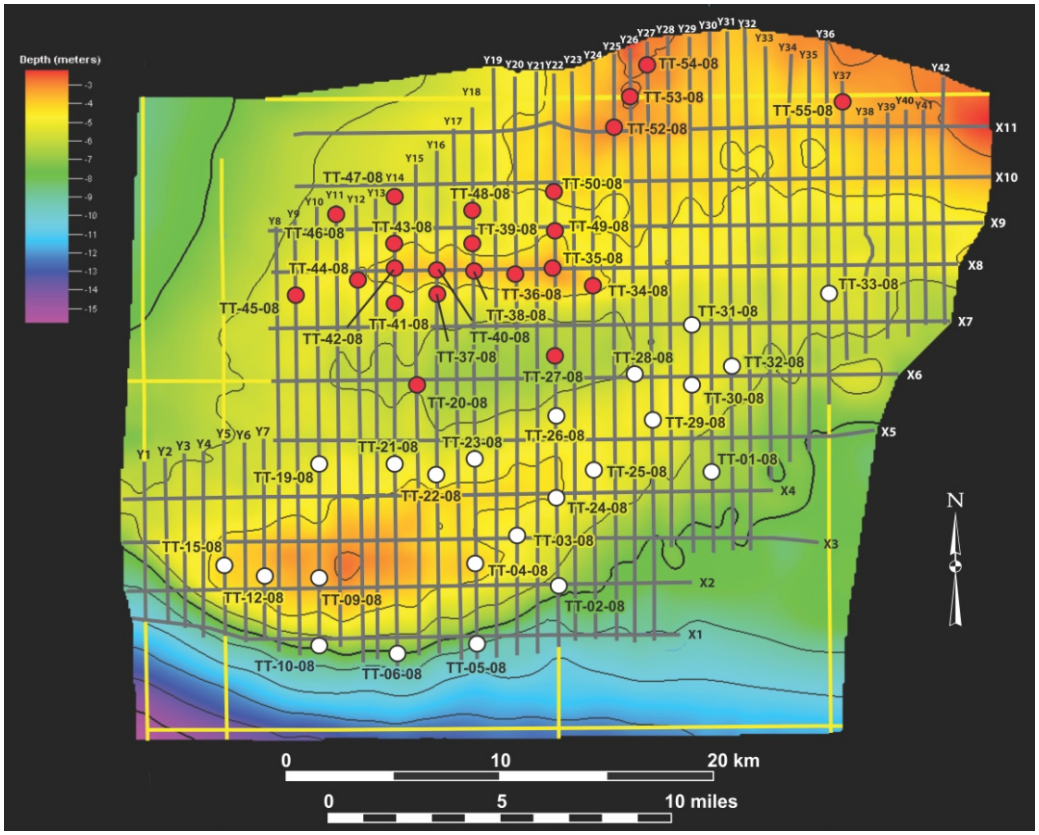

Figure 5. This figure illustrates the survey grid along which high resolution acoustic data were collected. The locations of 46 vibracores are also shown.

Survey Vessel – RV Coastal Profiler

The 2007 survey of Tiger and Trinity Shoals was accomplished using the R/V Coastal Profiler. Figure 6 shows this vessel which has an overall length of 41 ft (12.5 m) and a beam of 17 ft (5.2 m). The Profiler is a Lafitte Skiff style vessel designed primarily for shallow water operations. This vessel was custom built for shallow water geophysical data acquisition and vibracoring. Special ribbing and other supports were included in the construction to accommodate lifting heavy loads and withstanding substantial sea states. Booms, davits, and winches were custom built and located on the vessel at optimal sites for towing a variety of data-collection systems. The cabin was built to specifications for accommodation of our computer-based data acquisition units. Two 450 hp Catepillar (model 3126 B) engines power the Profiler. The vessel is equipped with a Simrad Auto Pilot which is essential for running straight survey lines. A 750 gallon fuel tank provides the capacity to run several days without refueling. The hull design and two diesel engines allows us to quickly run to the field sites (cruising speed ~ 22 kts). The Profiler can work comfortably on the continental shelf as well as in Louisiana's shallow bays to a water depth of < 3 ft (1 m).

A high resolution (reconnaissance-level) acoustic data collection survey was conducted in August 2007 using this custom built survey vessel. The purpose of the survey was to produce datasets on which an assessment of sand volume in Tiger and Trinity Shoal that would be available for coastal restoration considering industry infrastructure (oil and gas pipelines and production facilities) in the area in accordance with the guidelines established by Khalil (2004, 2008) and Khalil et al. (2010). Magnetometer data were collected simultaneously with side-scan sonar data, chirp sonar subbottom profiles, and bathymetry using standard procedures for shallow marine geophysical surveys (Roberts et al., 1999; Roberts et al, 2000). The magnetometer was deployed approximately 100 ft (30 m) off the stern of the survey vessel. A full spectrum subbottom profiler was deployed just below the waterline on the starboard around mid-vessel position. The side-scan fish was deployed on a bowsprit 5 ft (1.5 m) ahead of the vessel. This configuration mitigates vessel related noise in the acoustic data. Geographical coordinates were recorded for all the geophysical data collected, which was essential for integration of the various data sets.

Bathymetry

Bathymetry data were acquired using an Odom "HydroTrac" precision depth recorder. These data were recorded digitally along with other survey datasets. Offset of the transducer below the waterline was set at 20 in (50 cm). This offset was incorporated into the bathymetric data. No sound velocity data were acquired because of the shallow water depths in the survey area. Water depths were generally less than 16 – 26 ft (5-8 m).

Two separate data sets collected during geophysical surveys were used to separately map bathymetry. The primary bathymetric map was constructed using fathometer data. These data were imported into ArcGIS, and outliers were identified based on surrounding data points and deleted. Next, data were corrected for tidal fluctuations. Corrections were in reference to NOAA tidal station 8766072, located at Freshwater Canal Locks, Louisiana. Kriging interpolation was then performed on the corrected data within ArcGIS, and a final bathymetric map was produced.

Another bathymetric map was constructed using chirp seismic data. For each individual seismic line, the sea-bottom surface, easily interpreted when analyzing seismic, was manually traced within Petrel™ software. Using these sea-bottom seismic interpretations as input, a sea-bottom surface map was created within Petrel™ by interpolation. However, the z-axis of seismic data, and therefore the newly created sea-bottom surface map, is in the time domain (as opposed to true depth). By constructing a velocity model for the study area, a relatively simple domain conversion (i.e. time to depth) is performed within Petrel™, and a bathymetric map is generated.

Figure 6. The R/V Coastal Profiler, a custom built vessel for shallow water geophysical survey work and coring. This vessel was used for data collection in both the August 2007 and October-November 2008 surveys.

Side-Scan Sonar

Side-scan sonar efficiently maps the water bottom, producing an image of the various features and large changes in sediment texture that occur there. Side-scan data show reflection amplitudes from acoustic energy output by the side-scan fish and reflected back from the water bottom. Bottom features such as sand waves and ripples are clearly imaged in side-scan data. Also, differences in bottom sediment types can be distinguished from reflection amplitude

signatures. With ground truth calibration, discrimination and identification of bottom sediments, such as sand versus clay, is possible from reflection differences (Allen et al., 2005).Reflection amplitude signatures translate into various gray tones on a gray scale that have meaning regarding general grain size of sediments.

Although side-scan data are much less important to the Tiger-Trinity Shoals study than subbottom profiling, the data were collected simultaneously with other datasets. These data were acquired during the 2007 survey simultaneously on port and starboard channels using a Klein model 2260NV digital dual frequency (100 kHz/500 kHz) tow fish and a high fidelity, low loss armored single conductor coaxial tow cable, according to methods described in Roberts et al (1991), Roberts et al 2000, and Allen et al. (2005). Isis software was used for data acquisition and processing (Version 6.9.29.0, Triton Elics International Inc.). The side-scan sonar data were processed using parameter settings from previous surveys that have proved optimal for imaging sand-rich water bottoms. Slant, layback, and boat speed corrections were made with data collected during side-scan data acquisition. For these analyses, the 200 kHz channel data were used. This frequency provides adequate spatial surface resolution for imaging the sandy seafloor of the shoals. The individual side-scan lines were converted to a georeferenced TIFF image with 0.2 m (0.7 ft) resolution in both latitude and longitude for representing the characteristics of the shoal surface.

Subbottom Profiler

High frequency chirp subbottom profiling systems produce high resolution imaging of the shallow subsurface without strong "multiples" associated with other high resolution seismic sources such as boomers and sparkers. This feature makes the chirp sonar an ideal tool for imaging the shallow subsurface in sand searches. Different sediment types reflect the acoustic signal with different strengths which are recorded in the chirp data. Therefore, bottom "hardness" can be interpreted from the amplitude of the sediment-water interface or initial bottom reflector. Subbottom data are useful for: 1) discrimination of shallow subsurface stratigraphy, different sediment types, and interpretation of deposition and erosion; and 2) improving the interpretation of geological controls of surface reflectance (side-scan sonar) data.

The EdgeTech SB512i towfish (frequency of 5-12 kHz) and Model FS 5B Signal Processor constitutes the chirp sonar system used on the 2007 survey (Figure 7). The subbottom data were acquired by selecting the frequency range of 2-12 kHz at 20 ms. This system is augmented with a CODA DA50 portable computer-based seismic data acquisition system. The system is equipped with a FSSB Network Interface, an analog acquisition card (for use with any analog SBP system), internal 60GB hard drive, and a DVD-RAM storage drive. The CODA Geosurvey Windows Office Replay software were used as a digital data acquisition system and for displaying the data in real-time during the acquisition phase.

Subbottom data were saved in the industry standard SEG-Y format. Navigational data were retained for each shotpoint in the SEG-Y data.

Magnetometer

One of the most important datasets on Tiger-Trinity Shoals was the position and strength of magnetic anomalies. These data define oil and gas infrastructure and isolated metallic objects that influence the places where sand resources may be extracted if needed for coastal restoration purposes. A Geometrics Model G-882 marine cesium magnetometer was used on the Tiger-Trinity Shoal survey. The cesium magnetometer sensor and associated electronics modules are housed in a waterproof non-magnetic fiberglass tow body approximately 5 ft (1.5 m) length (Figure 8). This tow body or "fish" is easy to deploy and is equipped with 200 ft (61 m) of tow cable. The system has Maglog software which allows the operator to receive, display, and otherwise manage data from the fish on a PC. In addition, this software allows for integration of magnetometer data with GPS-derived location data.

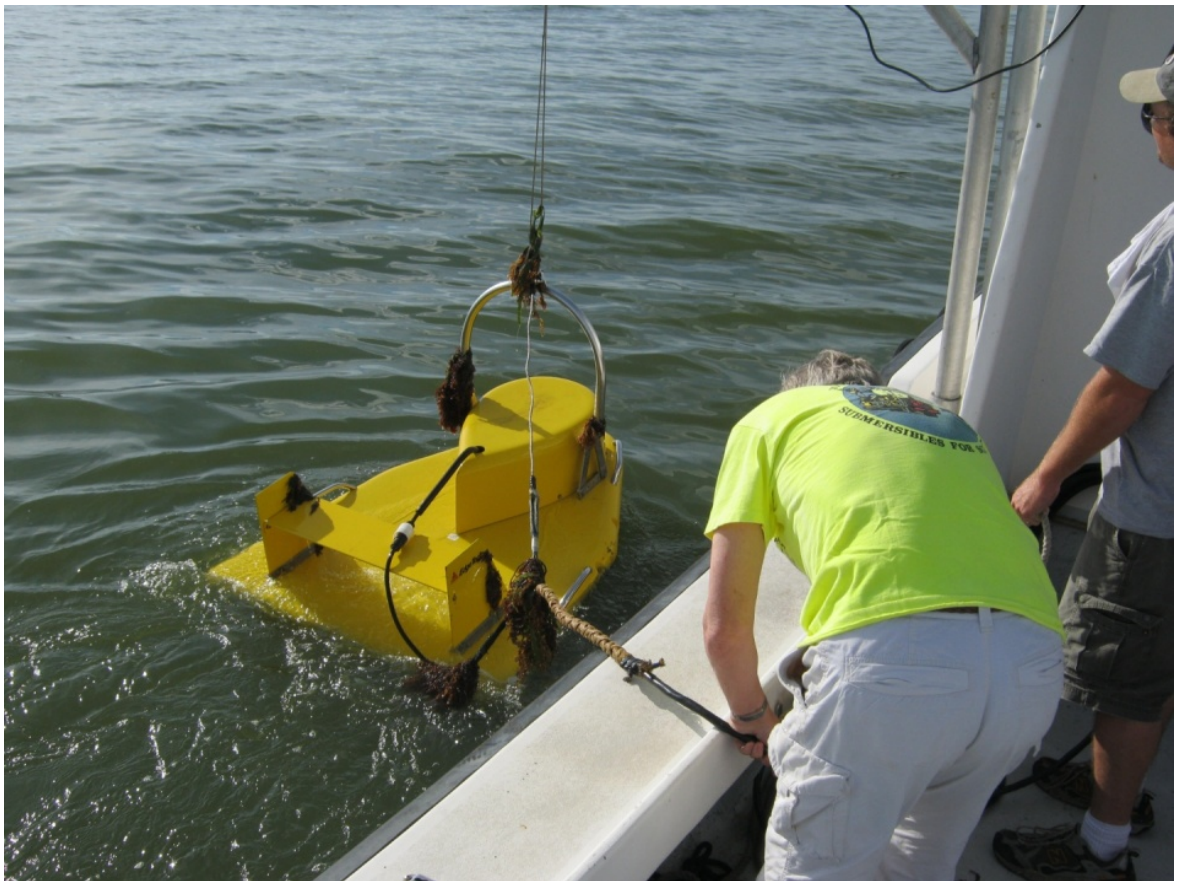

Figure 7. On the Tiger and Trinity Shoals survey, the EdgeTech SB512i towfish was deployed from a davit on the port side of the RV Coastal Profiler. This tow-fish rides efficiently in the water and was towed about 1.5 ft (~ 45 cm) beneath the water surface.

Figure 8. The Geometrics G-M882 Mini-Marine Cesium Magnetometer shown in this photograph is easy to deploy and retrieve from a small vessel like the RV Coastal Profiler.

Before the 2007, survey the Geometrics G-88 Mini-Marine Cesium Magnetometer System was acquired from Geometrics Inc., of San Jose, California. Prior to going in the field, the Coastal Studies Institute Field Support Group personnel spent mobilization time making sure all its systems were functional. As will be discussed in the results section of this report, the data acquired using this system were excellent and required only standard signal processing to identify "true" magnetic anomalies from noise spikes. The Geometrics Model G-M882 system was used with great success during the 2007 survey. It is easy to deploy and retrieve and produces low-noise results.

The raw magnetometer data files were exported as text files to the Geometric software Magmap 2000 and the significant anomalies were flagged. The positions of these flagged anomalies were exported as text files and then imported into ArcGIS for mapping purposes. The offset related to magnetometer sensor position relative to the GPS antenna location on the vessel ("layback") was calculated for each flagged position exported to ArcGIS. The magnetic anomalies were tabulated and then plotted along the ship tracks. The tracklines and magnetic anomalies were plotted over the locations of known magnetic infrastructure (pipelines and production facilities) in the survey area.

Vibracorer

Sediments and the stratigraphy of Tiger and Trinity Shoals were sampled using a marine vibracoring system operated from the RV Coastal Profiler (Figure 9). This vibracoring system

was custom built for Coastal Studies Institute by Dr. Charles Phipps of SEAS Vibracoring Systems of Australia. This durable system is made largely of aluminum to reduce handling weight. The motor drives eccentric counter weights in an O-ring sealed housing. The system is built for the challenging conditions associated with collecting multiple cores over extended sampling programs. Cores are taken in 3 in (7.6 cm) diameter aluminum irrigation tubing fitted with a custom built stainless steel core catcher. The unit used in the Tiger and Trinity Shoals investigation was capable of taking cores up to 15 ft. (4.5 m) long. Table 1 indicates the core identification numbers and locations of all vibracores collected during the 2008 field season.

Table 1.
Locations of Vibracores

Vibracore	Latitude	Longitude		Vibracore	Latitude	Longitude
TT-01-08	29.23892	92.08697		TT-32-08	29.28365	92.07793
TT-02-08	29.19278	92.16083		TT-33-08	29.31280	92.03136
TT-03-08	29.21300	92.18014		TT-34-08	29.31612	92.14284
TT-04-08	29.20082	92.19955		TT-35-08	29.32444	92.16243
TT-05-08	29.16924	92.19938		TT-36-08	29.32184	92.17962
TT-06-08	29.16533	92.23716		TT-37-08	29.31444	92.21732
TT-09-08	29.19589	92.27375		TT-38-08	29.32334	92.19961
TT-10-08	29.16853	92.27346		TT-39-08	29.33462	92.19965
TT-12-08	29.19618	92.29966		TT-40-08	29.32454	92.21744
TT-15-08	29.20148	92.31827		TT-41-08	29.31015	92.23724
TT-19-08	29.24300	92.27391		TT-42-08	29.32518	92.23689
TT-20-08	29.27659	92.22664		TT-43-08	29.33496	92.23698
TT-21-08	29.24195	92.23698		TT-44-08	29.32114	92.25467
TT-22-08	29.23901	92.21818		TT-45-08	29.31391	92.28336
TT-23-08	29.24661	92.19936		TT-46-08	29.34788	92.26471
TT-24-08	29.22933	92.16075		TT-47-08	29.35644	92.23680
TT-25-08	29.24072	92.14270		TT-48-08	29.34781	92.19959
TT-26-08	29.26352	92.16067		TT-49-08	29.33973	92.16071
TT-27-08	29.28799	92.16049		TT-50-08	29.35538	92.16046
TT-28-08	29.28086	92.12433		TT-52-08	29.38222	92.13276
TT-29-08	29.26038	92.11538		TT-53-08	29.39510	92.12484
TT-30-08	29.27443	92.09688		TT-54-08	29.40927	92.11652
TT-31-08	29.30128	92.09709		TT-55-08	29.39216	92.02358

Navigation

Geographical coordinates were recorded for all the geophysical data and vibracores collected. These data are essential for integration of the all survey data sets. Navigation data were acquired using a C&C Technologies GPS receiver system utilizing SatLoc3 differential GPS that produces sub-meter accuracy. The navigational data were delivered in real-time and these data were incorporated into the magnetometer, echo sounder, side-scan sonar, and chirp

sonar subbottom digital data sets. The GPS-fix data were sent to the data acquisition systems at a rate of one fix per second. Navigational control was maintained on an IBM compatible PC running HYPACK 2010® navigational software. A navigational chart with the plot of the survey plan was displayed along with the vessel's position, orientation, course, and speed. In addition, similar GPS location data were acquired at each vibracore site.

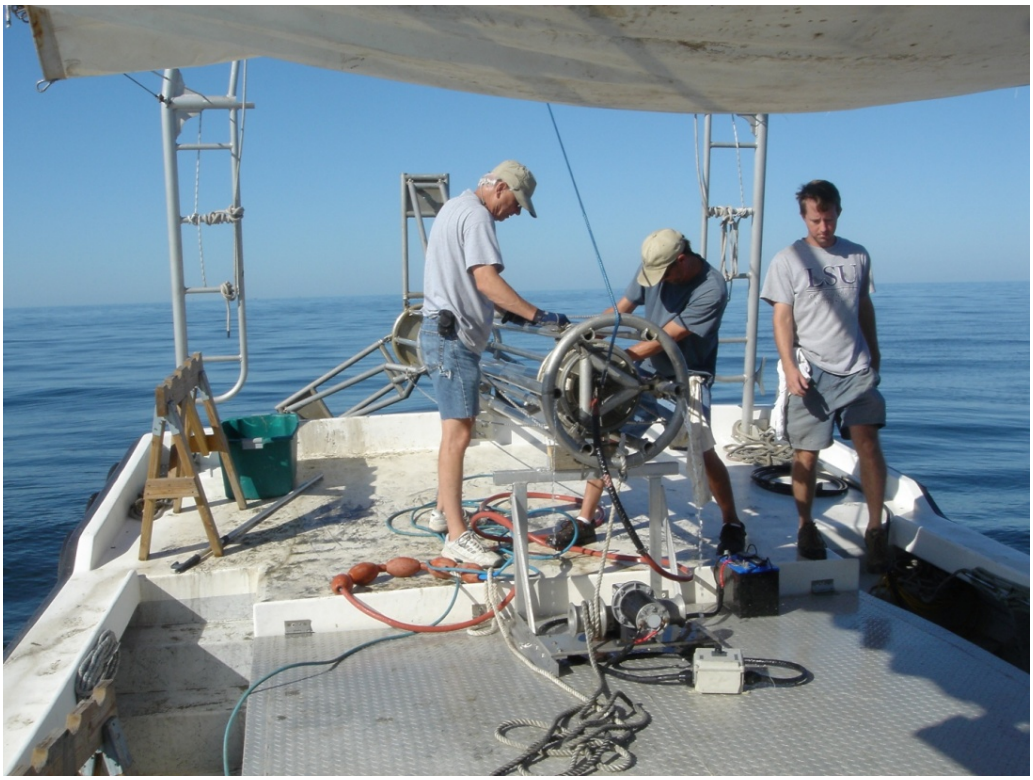

Figure 9. The custom built marine vibracoring system shown in this picture was used on the Coastal Profiler to collect vibracores up to a maximum of 15 ft. (4.5 m) long.

Grain Size Analysis

Grain-size analysis was conducted on the sand fraction of sediment samples collected from each vibracorer. For each sample the sand and mud fractions were separated by wet-sieving. Separated fractions were oven dried. Sand-mud ratios were subsequently determined. Afterwards, the sand fraction was dry-sieved using a Gilson SS-3 sieve shaker, at 0.25 phi (φ) sieve intervals. Table 2 depicts the standard subdivisions of sand-sized grain particles that were used in our investigation. Sands retained on individual sieves were weighed, and resulting data were entered into SediGraph 5100 software for analysis.

SediGraph software reports several statistics that describe the central tendency of a sample, including mean, mode, median, standard deviation, skewness, and kurtosis. In addition, it generates a particle-size table and a mass frequency vs. diameter histogram for each sample. See Appendixes 4-49, respectively, for grain-size analysis and sand-mud ratio results. Note that particle diameters are reported in micrometers (μm). See Table 2 for a sieve, micron, phi, or class conversion.

Table 2.
Grain Size Conversion Data

Sieve Mesh #	Millimeters	Microns	Phi (ϕ)	Wentworth Size Class
12	1.68	1680	-0.75	Very- Coarse Sand
14	1.41	1410	-0.5	
16	1.19	1190	-0.25	
18	1.00	1000	0.0	
20	0.84	840	0.25	Coarse Sand
25	0.71	710	0.5	
30	0.59	590	0.75	
35	0.50	500	1.0	
40	0.42	420	1.25	Medium Sand
45	0.35	350	1.5	
50	0.30	300	1.75	
60	0.25	250	2.0	
70	0.21	210	2.25	Fine Sand
80	0.177	177	2.5	
100	0.149	149	2.75	
120	0.125	125	3.0	
140	0.105	105	3.25	Very-Fine Sand
170	0.088	88	3.5	
200	0.074	74	3.75	
230	0.0625	62.5	4.0	

Modified from Folk (1974)

GeoTek Multisensor Core Logging

This new system for logging the geophysical properties of sediment cores allows both whole cores and split cores to be measured in a nondestructive fashion (Schultheiss and Weaver, 1992; Schultheiss and McPhail, 1989). The current sensor configuration measures (a) bulk density (using gamma-ray attenuation), (b) magnetic susceptibility at user-defined sample intervals down the core, (c) electrical resistivity, and (d) compressional (P) wave velocity (500 kHz). The multisensor core logger profiles presented with the vibracore photographs, lithologic log, and grain size data (Appendices of this report) are the gamma density (bulk density), p-wave velocity, and impedance (a calculated value). Split-core logging may provide slightly more reliable results than whole core logging as it mostly eliminates core-slumping effects that can lead to spurious results; it also gives higher resolution magnetic susceptibility readings. However, in most cases splitting the core may not be practical because of other demands such as geotechnical work.

In addition to the sensors mentioned above, the GeoTek multisensor core logger is equipped with a high resolution scanning digital camera. The core photographs that appear in the appendices of this report were made with the GeoTek scanning digital camera.

Bulk Density: Density is determined by measuring the attenuation of gamma rays through the core. A ^{137}Cs gamma source in a lead shield, with optional 2.5 mm or 5 mm collimators, provides a thin gamma beam which passes through the core. An integrated gamma detector measures the intensity of the beam relative to standards providing the gamma density of the core material. Density can be measured with an accuracy better than 1% depending upon count time used and core condition. Calibration standards are machined from a standard aluminum billet and stepped to enable calibration equations to be determined. Separate calibration samples are matched to each type of core liner used.

P-Wave Velocity: Compressional wave speed measurements are conducted using two 250-500 kHz piezo-electric ceramic transducers which are spring-loaded against the sample. Measurements are accurate to about 0.2%, depending on core condition. The ARC (Acoustic Rolling Contact) transducer uses a stationary active transducer element, which is made from a 1-3 Polymer Composite, in which the PZT material comprises a forest of narrow longitudinal rods embedded in a polymer. This material combines high coupling with relatively low acoustic impedance.

The transducer takes full advantage of these properties by including a front coupling layer and multi-layer composite backing to suppress unwanted internal ringing and back radiation. This multi-layer composite backing provides good acoustic loading and very high return losses, resulting in a unit with no detectable spurious internal modes and an extremely high back-to-front ratio (in excess of 60 dB).

The stationary composite element is surrounded by oil and a rotating soft deformable diaphragm. This arrangement enables the complete transducer assembly to rotate as the core is passed through the spring loaded opposing transducer pair. The careful internal design provides radiussed internal locating lips which gives a wide contact area and positive repeatable location of the transducers over core diameters within the range of 50 mm to 150 mm.

Impedance: Acoustic impedance is simply the product of density and velocity. Each individual layer within the earth has a unique impedance value, as each layer has a unique density and velocity. A change in impedance across an interface between separate layers causes a reflection of acoustic energy. A synthetic seismogram can be created by convolving reflectivity data with the seismic data. The synthetic seismogram can then be used to correlate seismic data with core data, thus improving interpretations (Liner, 2004). Bulk density and p-wave velocity from the multisensor core logger were used to construct the impedance profile presented in the appendices for each vibracore.

Multisensor Core Logger Data Editing: Raw sensor data were processed using calibration parameters to provide measurements in standard units of measurement for each sensor. For presentation purposes, the words “section break” were included on the MSCL profiles for those areas influenced by proximity of core endcaps, and obvious gaps in sediment visible through core liner. This influence is most significant for both p-wave and gamma density sensors.

Petrel Seismic Data Analysis Software

Schlumberger's Petrel™ software provides state-of-the-art computing applications primarily for the oil and gas industry. Petrel's™ capabilities include both 2D and 3D seismic interpretation, time-depth conversion, well correlation, stratigraphic interpretation, complex geologic modeling, property modeling, facies analysis, volume calculation, geologic mapping, among many others. Its advanced visualization capability allows the user to examine interpretations, whereas its geostatistical approach helps reduce uncertainty in those interpretations. This powerful software program was used to manage the seismic and vibracores data collected on Tiger and Trinity Shoals and to make calculations critical to the central theme of this project, estimates of sand available for coastal restoration purposes.

RESULTS

Data on which this report is based were collected during two stages, one for collection of geophysical data and the other for vibracoring. The geophysical data collection was conducted August 8-28, 2007 while the vibracores were acquired in three separate field trips during the period October 25 – November 19, 2008. Field operations were conducted from a camp at Cypremort Point owned by Mr. and Mrs. Ned Weeks. This base for our field operations made access to the study site on the inner continental shelf less than a two-hour trip using the RV Coastal Profiler with a crusing speed of slightly over 20 kts. Our base of operations was also close to a refueling station and reasonably near grocery and hardware stores in New Iberia.

After the Year 1 (2007) field season of collecting over 750 line mi (1200 line km) of high resolution subbottom, bathymetry, side-scan sonar, and magnetometer data our research time was spent in data reduction and analysis. The subbottom data were of particular importance in meeting the objectives of this investigation which focus on making estimates of the volume(s) of sand available in the Tiger-Trinity Shoals complex that may be available for extraction for coastal restoration projects. Once the 46 vibracores were taken during Year 2 of the project credible estimates of sand in the shoals could be calculated. The cores were logged with the GeoTek Core Logger, photographed, sampled and analyzed for grain size, and graphically logged. These data appear in the Appendices of this report.

In the following subdivisions of the Results section, the Tiger-Trinity Shoals will be interpreted in the context of providing new insight about these transgressive sand bodies that is important to evaluating their potential as sand resources for the State of Louisiana to eventually use for restoring our disappearing coastal environments.

Bathymetry

Figures 10A and B are bathymetric profiles of the Trinity and Tiger Shoals Complex. Figure 10A was generated using Petrel™ software from data gathered by manually tracing the sea-bottom surface of each seismic line acquired, and then interpolating between lines. The original bathymetric data set of 53 seismic lines was supplemented with additional seismic data gathered in the summer of 2010, which allowed us to extend the bathymetry further west and south (i.e. as compared with Figure 10B). Figure 10B was generated by ArcGIS using

fathometer data. Although, Figures 10A and B generally mimic each other, Figure 10B is considered more accurate: the fathometer was attached along the starboard side of the boat at a fixed depth (20 in or 50 cm beneath the sea surface while stationary), whereas the subbottom profiler was towed from the port side at a varying depth of 3-3.5 ft (1.0 – 1.5 m).

As Figures 10A and B reveal, Trinity Shoal is a concave landward depositional feature. It extends 22 mi (35 km) in length, and stretches as wide as 6 mi (~ 10 km) in width in its west-central region, before tapering off in an east, northeast direction. It has a relief of 13-16 ft (~ 4 – 5 m) in its southern perimeter, whereas it displays a relief of 3-6 ft (~ 1 – 2 m) to the north. In contrast, Tiger Shoal exhibits a more linear, shore-parallel orientation. Tiger Shoal stretches 16 mi (~25 km) in length, and has a maximum width of 3 mi (~ 5 km). Its bathymetric relief is 5-7 ft (~ 1.5 – 2.0 m) all sides, except to the northeast where it is slightly less. Further northeast of Tiger Shoal, bathymetry indicates shoals in a broad region to the north-northeast of the study area. In the central region of the study area is a bathymetric low, which is as deep as 21 ft (~ 6.5 m). It is bordered to the south and north by bathymetrically pronounced Trinity and Tiger Shoals, respectively, and to the east and west by relatively shallower waters. The shallowest sections of the study area are less than 10 ft (3 m) in depth, and occur at the crests of both shoals as well as in the northern region. The deepest sections of the study area occur south of Trinity Shoal. The relatively sharp dip in the bathymetry in this area signifies the transformation from the Trinity and Tiger Shoals Complex to the seaward-dipping continental shelf.

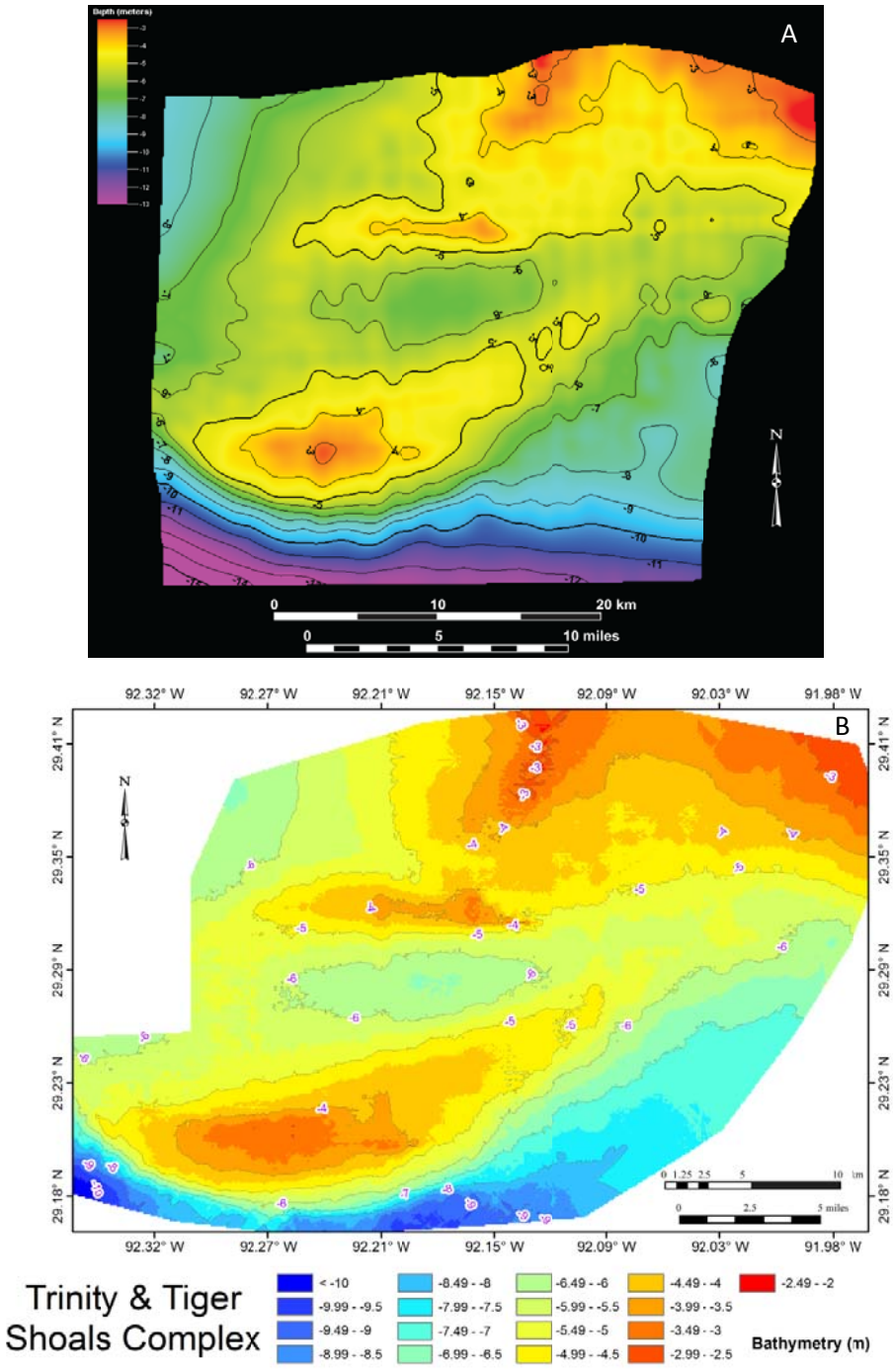

Figure 10. A) and B) are bathymetric maps of the Trinity and Tiger Shoals Complex. A) was compiled using data extracted from the geophysical data set of 2007 and parts of 2010, whereas fathometer data were used to generate B). Both figures similarly show distinct characteristics of the Trinity and Tiger Shoals Complex: 1) Trinity Shoal is much larger than Tiger Shoal; 2) A relatively deep bathymetric low lies between, and separates the two shoals; 3) north of Tiger Shoal, bathymetry shoals again and remains relatively shallow; and 4) water deepens to the south of Trinity Shoal, indicating the southern extent of the shoal complex.

Stratigraphic Framework and Lithostratigraphy

In addition to mapping the sea-bottom surface as described above, other major seismic reflectors were recognized and mapped within Petrel™. These mapped subbottom surfaces were in turn used as guides in selecting vibracoring locations. A strong motivation was to penetrate seismic surfaces in as many locations as possible, so as to integrate ground-truth core data with the geophysical data. After data integration, stratigraphic and geological interpretations were extrapolated across the study area, and a stratigraphic framework of the shoal complex was established. Lithologic (grain size) descriptions used in this part of the report are according to Folk (1974).

Interpreting the base of both shoals (i.e. the maximum subbottom extent of shoal sand) was critical in establishing both a sand-thickness map, and for calculating total sand volumes. In areas of Trinity Shoal that are relatively thin (i.e. < 20 ft or 6 m in thickness), mapping its base within Petrel™ was an easy task, as there is a distinct seismic reflection at the interface separating the overlying shoal sand from underlying muddy sediment. However, acoustic energy tends to attenuate in thick sands, with very little acoustic energy reflected from lithologic changes that underlie thick sand bodies (Jackson and Richardson, 2007). In such conditions within Trinity Shoal, the shoal base was mapped up to the point where the seismic reflector diminished. The interpreted shoal base was then extended beneath the shoal based on both the seismic reflector's geometry and lithologic data from Penland et al. (1990). In contrast, attenuation of acoustic energy due to thick sand deposits was not a problem associated with the thinner Tiger Shoal, and the mapping of Tiger Shoal's base was a relatively simple task. Based on the integration of lithological and seismic data, and interpretations determined from that integration, sand volume calculations and a sand-thickness map were generated for each shoal by geometrical modeling processes within Petrel™.

Figure 11 depicts the seismic profiles and vibracore locations selected to illustrate both the stratigraphic framework and lithologic character of the Trinity and Tiger Shoals. All discussion that refers to individual seismic lines and vibracores within this section is directed to Figures 12, 13, and 14. Tiger Shoal, the most northern of the two sand bodies, is a relatively clean, very-fine sand unit with some occasional shell and shell hash. However, within its most eastern region, sand particles as large as medium sand size occur, and shell content increases substantially. The sandy Tiger Shoal unit, which crops out at the sea bottom, overlies a sandy mud stratigraphic unit. This latter unit is characterized by frequent occurrences of sand lenses with intermittent sand layers and is highly bioturbated. Underlying this sandy-mud unit is a silty clay unit.

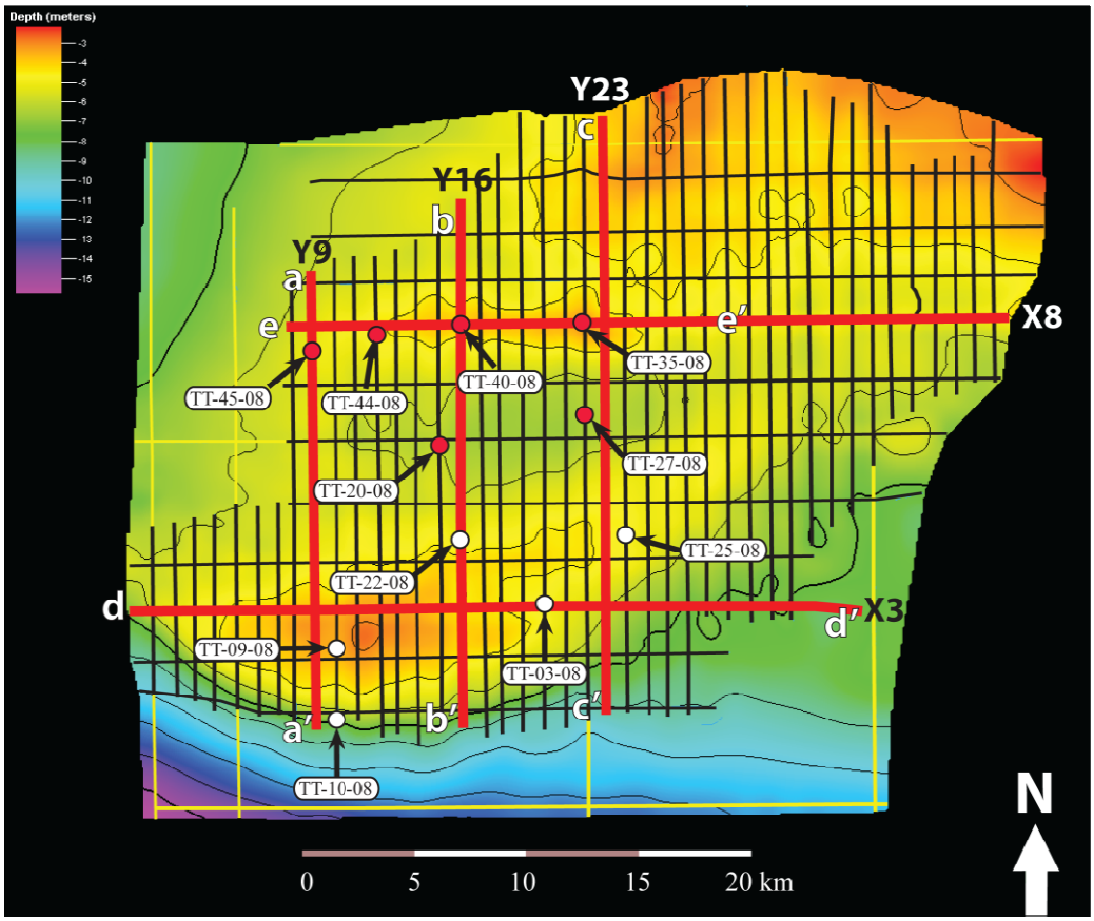

Figure 11. This figure illustrates the data collection grid with the five seismic tracklines and eleven vibracores identified that are discussed in the Stratigraphic Framework and Lithostratigraphy section of the report.

Seismic line X8, which extends east-west along the strike of Tiger Shoal, seismic lines Y16 and Y23, which both extend north-south in accord with the dip of Tiger Shoal, and vibracores TT-44-08, TT-40-08, and TT-35-08 demonstrate the above observations. The red horizon interpreted within seismic lines X8, Y16, and Y23 depicts the base of Tiger Shoal and, in effect, its areal extent. Tracking this horizon with respect to the sea-bottom surface reveals the, generally, geometrically symmetrical character of Tiger Shoal, whereas the upper stratigraphic unit present in all three vibracores depicts Tiger Shoal's sandy lithology. Though vibracore TT-35-08 does not penetrate the red horizon, both vibracores TT-40-08 and TT-44-08 do. This seismic interface correlates with the lithologic interface, as seen in the two vibracores, that separates the overlying Tiger Shoal sandy unit from the underlying sandy-mud unit. Both vibracores also penetrate the deeper seismic interface that is delineated in purple. The lithologic change that occurs within these cores separating the overlying sandy-mud unit and the underlying clay unit corresponds with this seismic interface.

Trinity Shoal is a relatively clean, sandy body composed of very-fine grained sand with sporadic occurrences of shell and shell hash, and like Tiger Shoal, this stratigraphic unit crops

out at the sea bottom. Trinity Shoal is very thick in some areas, and consequently, data beneath the shoal in those areas is poor or nonexistent. Nevertheless, where Trinity Shoal thins, a similar sequence of stratigraphic units as identified in the Tiger Shoal region may be observed: a predominately sandy shoal unit overlies a sandy-mud unit that is characterized by frequent sand lenses, intermittent sand layers, and bioturbation, which itself, as observed in Trinity Shoal's northeast quadrant, overlies a clay unit.

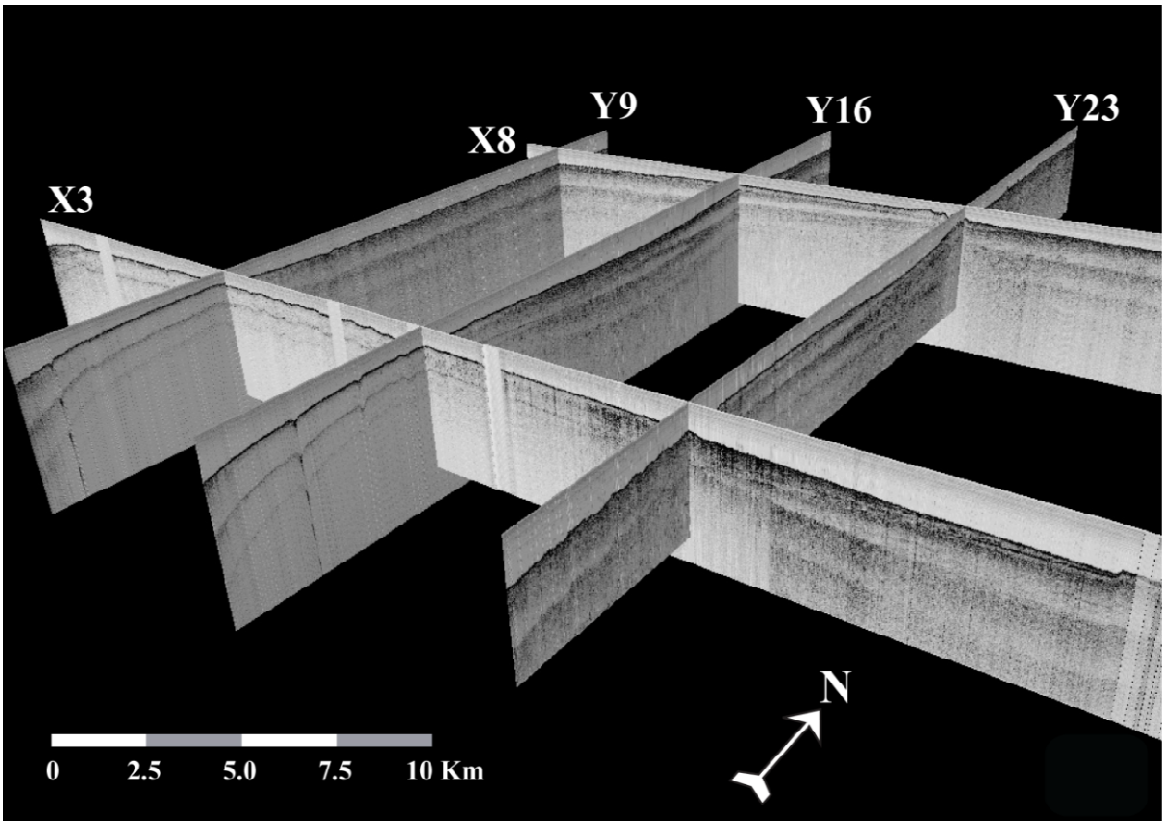

Figure 12. Five seismic lines viewed in 3D perspective using Petrel™ software comprise this figure. These lines illustrate the stratigraphic framework of the Tiger and Trinity Shoal Complex.

These observations of Trinity Shoal are illustrated by seismic line X3, which extends east-west along the strike of Trinity Shoal, seismic lines Y9, Y16, and Y23, which transect north-south in congruence with the dip of Trinity Shoal, and vibracores TT-03-08, TT-09-08, TT-22-08, TT-25-08, and TT-45-08. The interpreted seismic reflector defined yellow within these seismic lines depicts the base of Trinity Shoal. As seismic line Y9, Y16, and X3 illustrate, the Trinity Shoal stratigraphic unit is thick and bathymetrically pronounced within its southern region. The 14.5 ft (4.4 m) vibracore TT-09-08, located within this region and projected into seismic line Y9, consists of entirely very-fine sand to silty sand and, likewise, does not penetrate the yellow horizon. However, vibracore TT-10-08, which is projected into seismic line Y9 near it southern termination point, does penetrate the rapidly shallowing seismic reflector. This is affirmed from the shallow lithologic interface within this core that separates the overlying

Trinity Shoal unit with the underlying sandy mud. This rather abrupt termination of Trinity Shoal indicates its most southern extent.

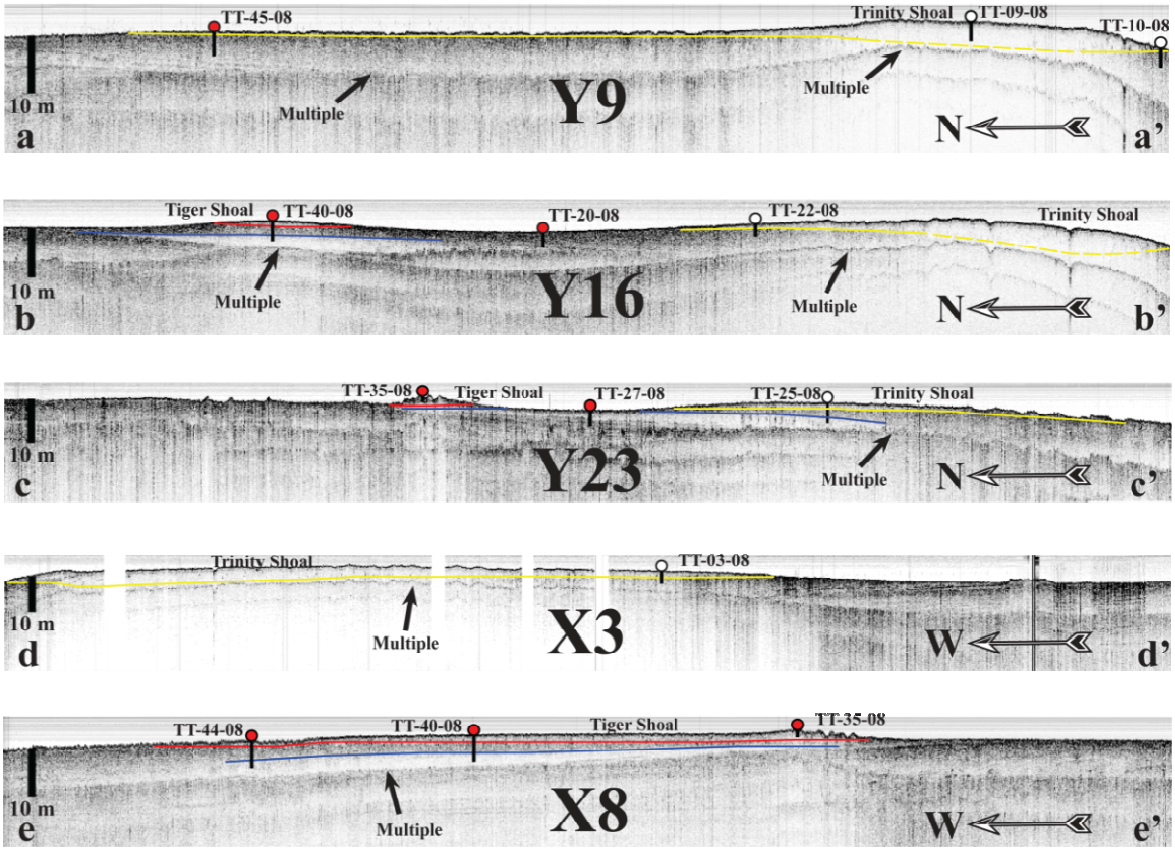

Figure 13. Five seismic lines (three north-south and two east-west) selected to illustrate the stratigraphic framework of the Trinity and Tiger Shoals Complex. Key seismic reflectors are interpreted in color. Core locations with their approximate penetration depths are depicted. Note that only a part of seismic line X8 is shown here, so that the relatively thin Tiger Shoal is more discernable; note that e' (see Fig. 11) depicts where seismic line X8 ends. Vertical exaggeration is 100X.

In contrast to Trinity Shoal's most southern region, its northern region is characterized by thinning transgressive sands that encompass a broader area. This northern region can be further subdivided into three areas: a vast sand sheet that protrudes from the northwest quadrant, a sand body that tapers to the northeast, and a relatively narrow transgressive sand that lies between the two. The sand body that protrudes from Trinity Shoal's northwest quadrant is depicted in seismic line Y9. The base of Trinity Shoal, as the yellow horizon illustrates, extends far north as a thin transgressive sand sheet, where it terminates by welding to the west flank of Tiger Shoal. The yellow seismic reflector is penetrated in this region by vibracore TT-45-08. The lithologic interface recognized within this core at 3.3 ft (~ 1 m) subbottom separates the overlying sandy Trinity Shoal unit and the underlying sandy-mud unit, which likewise correlates with the yellow seismic reflector. To the east, along the transect of seismic line Y16, the interpreted yellow seismic reflector signifies that the transgressive sand component of Trinity Shoal is relatively

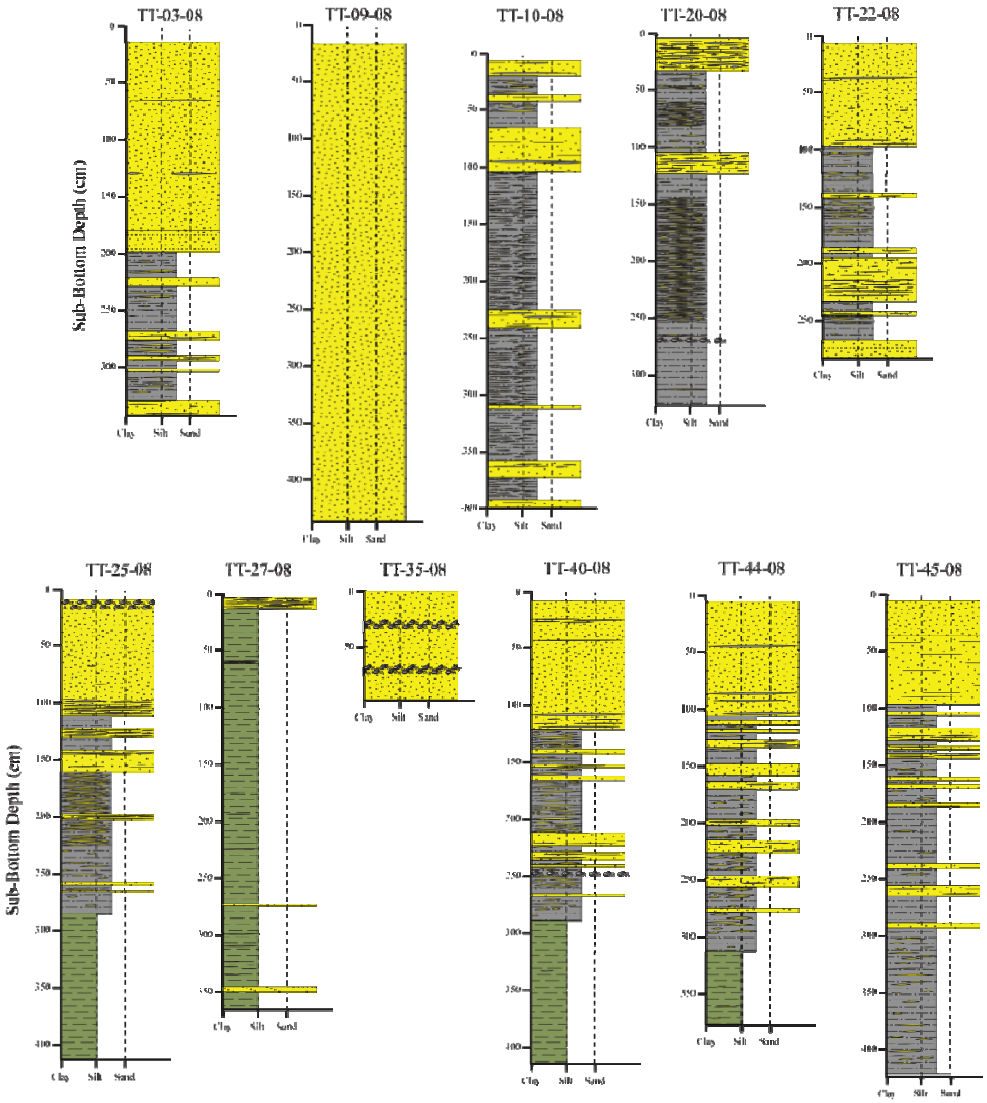

Figure 14. Lithologic logs of vibracores cited in Figure 13.

narrow. Vibracore TT-22-08 corroborates this seismic interpretation, as the lithologic interface separating the overlying shoal unit and the underlying sandy-mud unit correlates with the yellow horizon. That part of Trinity Shoal that tapers to the northeast can be first perceived in seismic line X3, in the vicinity of vibracore TT-03-08. This core penetrates through the major seismic reflector delineated yellow (Fig. 13), which, again, correlates with the lithologic interface that separates the overlying Trinity Shoal unit and the underlying sandy mud unit. This same stratigraphic sequence, concurrent with a northeast trending, thinning Trinity Shoal, is observed further to the northeast in seismic line Y23 and vibracore TT-25-08 (which is projected into seismic line Y23). Not only does this vibracore penetrate the yellow horizon but also the deeper horizon delineated red (Fig. 13). This red horizon correlates with the lithologic interface observed within vibracore TT-25-08 that separates the middle stratigraphic unit (i.e. the sandy mud) from the underlying clay unit. This clay unit is the same unit that was recognized in the Tiger Shoal region.

Seismic lines Y16 and Y23, and the seismic interpretations therein, clearly demonstrate that Trinity and Tiger Shoals are separate depositional units; bathymetric profiles from these seismic lines alone would suggest this. Further evidence is presented by vibracores TT-20-08 and TT-27-08, which are projected into seismic lines Y16 and Y23, respectively, and are both considered positioned, geographically, between the two shoals. The sand at the top of vibracore TT-20-08 very likely was introduced from Trinity Shoal. However, this muddy-sand layer is not considered a part of the clean transgressive sand sheet flanking the north side of Trinity Shoal. Nevertheless, the sandy-mud stratigraphy that underlies this thick muddy sand confirms that Trinity and Tiger Shoal are separate sand bodies. Similarly, a muddy-sand layer lies at the top of vibracore TT-27-08, and likewise it is not considered a part of Trinity Shoal. Drawing the same conclusion as above, the clay unit that underlies the thin muddy-sand unit clearly demonstrates that Trinity and Tiger Shoals are separate depositional unit.

Sediment Characteristics

The grain size of the sand fraction of Trinity Shoal is entirely very-fine sand (0.062-0.125 mm). Though no real trend exists in the central portion of Trinity Shoal (see TT-09-08, TT-12-08, TT-15-08), the shoal's overall areal trend in grain size distribution is generally coarsening in the east, northeast direction. The reader can observe this trend by following two transects: beginning at TT-04-08 and ending at TT-32-08 and likewise, within the thin backside of the shoal beginning with TT-19-08 and ending with TT-28-08. In fact, the sand fraction in the eastern quadrant of Trinity Shoal approaches the fine-sand grain size. The sand fraction also generally coarsens upwards, although no coherent vertical trends were detected in TT-09-08 and TT-15-08, and TT-04-08 actually coarsens downwards. One final interesting grain-size pattern observed in Trinity Shoal is the generally fining trend from a southeast to northwest direction. This trend can be observed in the following short transects: TT-30-28 to TT-28-08; TT-29-08 to TT-28-08; TT-25-08 to TT-26-08; TT-24-08 to TT-23-08. However, this trend breaks down in TT-03-08 to TT-23-08 or from TT-04-08 to TT-22-08. In addition to the generally coarsening upwards of grain size, the observation of an approximate fining in the northwest direction conceivably reflects the dominant wind and wave direction, and therefore the dominant direction of sediment transport that characterizes the northern Gulf of Mexico.

Unlike Trinity Shoal, Tiger Shoal exhibits some heterogeneity in its sand fraction: grain size ranges from very-fine to medium sand, and in some cases is bimodal. However, all of this heterogeneity is found in Tiger Shoal's most eastern section (see TT-34-08, TT-35-08, TT-49-08; Figure 5). To the west of this area, the sand fraction of Tiger Shoal is entirely very-fine sand (0.076-0.123 mm). The overall areal trend in grain-size distribution coarsens to the east. This trend is indicated by the following transect: beginning with TT-44-08 and ending with TT-34-08. Down-core in the sand fraction cannot be generalized, as there is no vertical consistency among cores within Tiger Shoal. Like Trinity Shoal, Tiger Shoal reveals a generally fining trend from a southeast to the northwest direction, which is determined from the short transects TT-36-08 to TT-39-08, TT-40-08 to TT-43-08, and TT-37-08 to TT-42-08. However, the directly south to north transect of TT-38-08 to TT-39-08 does not follow this trend. Nevertheless, the overall fining to the west of the sand fraction and a similar trend in a southeast to northwest direction conceivably reflects the dominant direction of sediment transport diagnostic of the northern Gulf of Mexico.

Sand Thickness and Total Sand Volumes

Figure 15 is a sand-thickness map of the Trinity and Tiger Shoals Complex, revealing obvious spatial and volumetric differences between the two shoals. The thickest sand deposits occur within Trinity Shoal's southern region, with a maximum thickness of 7+ m. To the immediate south of this area, the most southern extent of the study area, shoal sands thin considerably. This indicates both the southern limit of Trinity Shoal and, in some cases, the southern limit of seismic coverage. However, where coverage is limited, adjacent areas are not, and overall coverage is considered adequate. In contrast, sands thin less dramatically over the broader northern region of Trinity Shoal, a likely expression of landward sand migration under transgressive processes. Toward the northeast, sands progressively taper off to an end point, which generally mimics Trinity Shoal's bathymetric profile (see Fig. 10). However, speculating sand thickness by bathymetry alone could be slightly misleading within the study area's western section: seismic interpretations indicate that Trinity Shoal is associated with a progressively thinning body of sand that extends landward from its western quadrant, ultimately welding to Tiger Shoal.

Tiger Shoal, in contrast, is a more linear, symmetrical body of sand. Maximum sand thickness is 6.5 ft (2+ m), and thins approximately proportionate along its north, east, and southern perimeters. However, Tiger Shoal appears to slightly expand a thin sand sheet toward the west, northwest, where it welds to the northwestern boundary of Trinity Shoal.

The isopach map generated herein deviates sharply in some respects from the previous interpretation by Penland et al. (1990). One difference is the location of the thickest sand deposits within Trinity Shoal. We interpreted these to be located within the shoal's most southern extent, whereas the previous study positioned them further north. Moreover, unlike the previous study, we did not interpret sand thicknesses to exceed 26 ft (8 m). But the most critical difference between our findings and those of the previous study was our respective interpretations of the sand sheet protruding from Trinity Shoal's northwest quadrant. We interpreted a relatively thin sand sheet (primarily ≤ 3 ft or 1 m) that diminishes at the latitude of Tiger Shoal, whereas Penland et al. (1990) depict a much thicker sand unit 6.5 – 20 ft (2-6 m) extending substantially north of Tiger Shoal. This latter discrepancy in findings between our respective studies primarily accounts for the conflicting estimations of overall sand volume (Table 3): Penland et al. (1990) advocate a sand volume for the Trinity and Tiger Shoals Complex that is 2.73 times greater than the sand volume we calculate.

Table 3
Sand Volumes: This Study vs Penland et al. (1990)

	Penland et al. (1990)	Roberts et al. (2010)
Total Sand Volume	2.6 billion yd^3 (2 billion m^3)	933.379.955 yd^3 (731,615,645 m^3
		Trinity 898,277,592 yd^3 (686,778,133 m^3
		Tiger 58,645,624 yd^3 (44,837,512 m^3

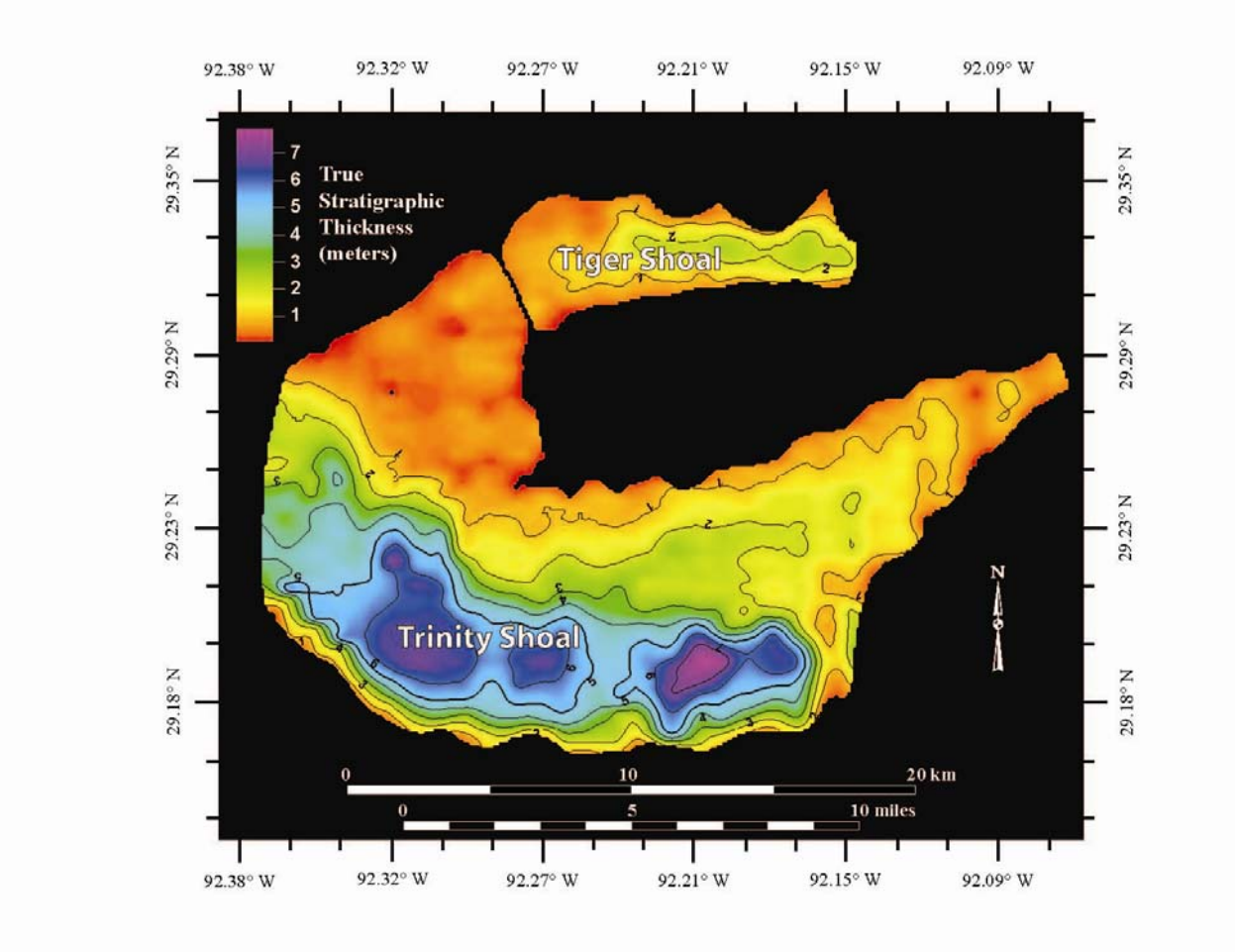

Figure 15. Isopach map of the Trinity and Tiger Shoals Complex. The thickest areas of Trinity Shoal are primarily in its most southern region, whereas Trinity Shoal gradually thins over its broader northern region. Tiger Shoal, in contrast, is more symmetrical in both sand distribution and thickness.

Infrastructure Constraints and Volumes of Extractable Sand

The Tiger and Trinity Shoals occupy an area of the inner continental shelf off the central Louisiana coast where the oil and gas industry has an active presence. Pipelines and production platforms that service this industry result in an infrastructure that constrains where sand stored in the shoals can be potentially extracted. Figure 16 illustrates the locations of these pipelines and production platforms in the shoal complex area as defined by magnetic anomalies. The linear distributions of these anomalies identify the pipelines which commonly intersect at production platforms. A table of all magnetic anomalies is presented in Appendix 50. This table not only assigns a latitude and longitude to each anomaly, but also provides a gamma reading (strength of the anomaly). In addition, Appendix 50 presents a large fold-out version of the anomaly map of Figure 16. Based on the work represented by this report, the State of Louisiana needs to substantially revise its polygons of significant sand resources to be protected in Notice To Lessees No. 2009-G04.

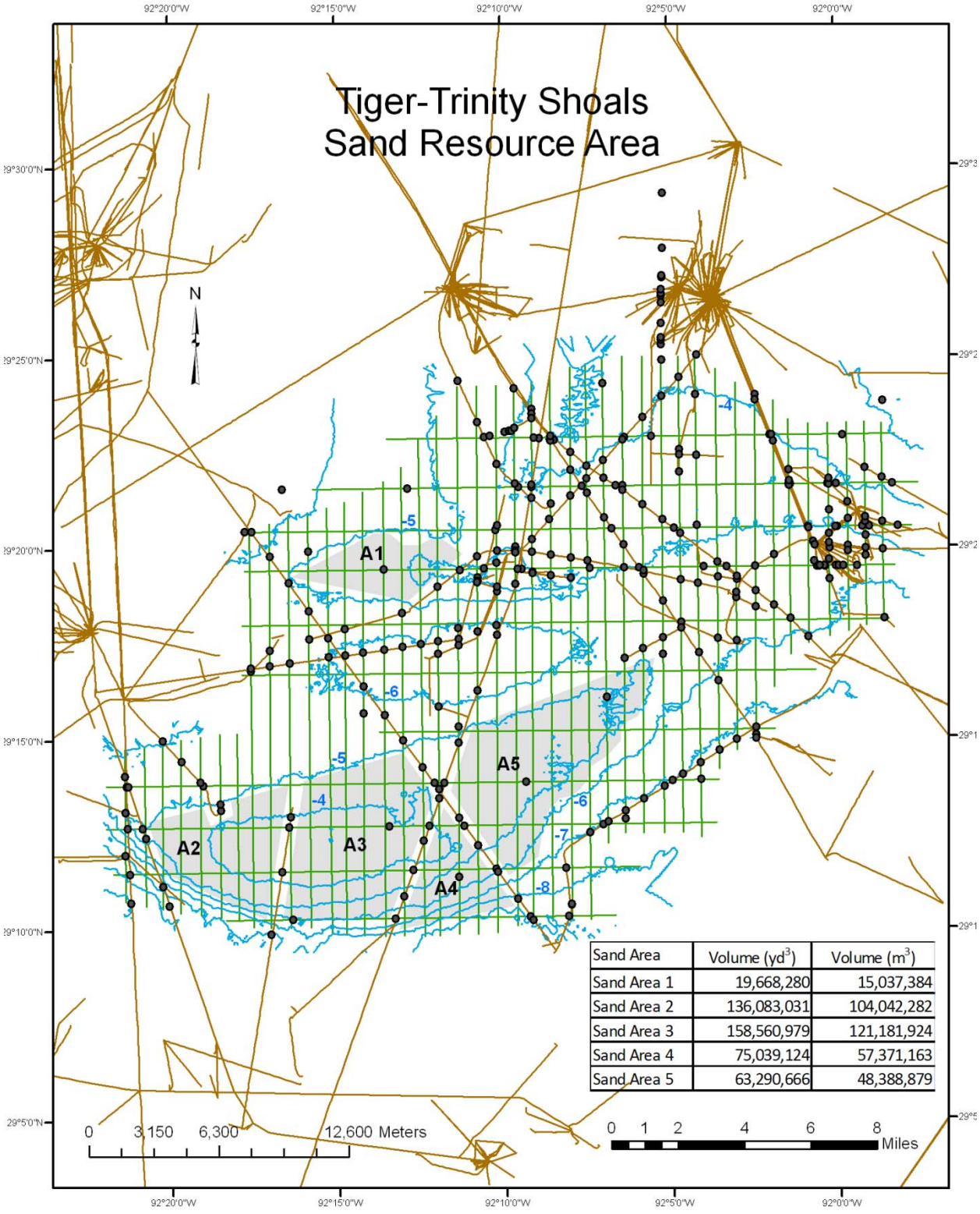

Figure 16. Areas of potential sand extraction considering the network of oil and gas pipelines and production platforms as well as significant magnetic anomalies.

Table 4
Sand Volumes in Areas Defined by Oil and Gas Infrastructure

Sand Area	Volume (yd^3)	Volume (m^3)	Grain Size
Sand Area 1	19,668,280	15,037,384	3.75 – 3.25 ϕ (0.0793 – 0.110 mm)
Sand Area 2	136,083,031	104,042,282	3.75 – 3.5 ϕ (0.0772 – 0.0894 mm)
Sand Area 3	158,560,979	121,181,924	4.0 – 3.5 ϕ (0.0739 – 0.0953 mm)
Sand Area 4	75,039,124	57,371,163	4.0 – 3.5 ϕ (0.0739 – 0.0937 mm)
Sand Area 5	63,290,666	48,388,879	3.75 – 3.25 ϕ (0.0784 – 0.121 mm)

Areas where sand could be potentially extracted are identified as shaded polygons on Figure 16. These five areas include both Tiger and Trinity Shoals. Table 4 summarizes the sand volumes calculated from each of the polygons using the Petrel™ software. The smallest volume of extractable sand is in Area 1, the western end of Tiger Shoal. Oil and gas infrastructure excludes the remainder of Tiger Shoal from being considered as a sand resource. By comparison, Trinity shoal has over 430 x 10^6 yd^3 (330 x 10^6 m^3) of sand in the four polygons that relate to this shoal, with the largest polygon (Area 3) having over 158 x 10^6 yd^3 (121 x 10^6 m^3) of potentially extractable sand. These areas were calculated using a buffer zone of 1000 ft (~ 305 m) from the pipelines that define them. Table 4 presents maximum volumes calculated from the lithostratigraphic data established by high resolution subbottom data and vibracores. Although the magnetic anomalies mostly define the pipelines in the shoal complex area, there are a few erratic magnetic anomalies that occur within the polygons that define areas where sand mining is possible. These anomalies have no pattern of occurrence and when compared to others that define the oil and gas infrastructure, they have small gamma deflections. Consequently, these anomalies are considered local metallic object such as anchors, small pieces of pipe, and other metallic debris probably associated with the oil and gas activity in the area.

CONCLUSIONS AND RECOMMENDATION

Geophysical datasets and vibracores collected during August 8-28, 2007 and October 25 – November 19, 2008 provide the most comprehensive database ever collected on the Tiger and Trinity Shoal Complex. These data were collected with the primary objective of assessing these two offshore shoals as potential sources of sand for future coastal restoration projects along the central Louisiana coast. This report presents the data as summary figures in the text and Appendices 1 to 50. Digital data files are recorded on a summary DVD (Appendix 51).

Previous geophysical data and vibracores collected on the Tiger and Trinity Shoal Complex, described in an earlier section of this report, proved that these shoals were sand-rich, but the deposits were relatively thin. Considering the regional nature of data collection associated with this 1980s project and the current growing need for sand for coastal restoration, a new appraisal of the sand resources in these shoals was needed. Critical datasets of this new evaluation of the shoals included high resolution subbottom profiles, vibracores, and magnetometer data. Approximately 750 line mi (> 1200 line km) of subbottom data provided the shallow subsurface stratigraphic framework and seismic facies that were calibrated to sediment types with the 46 vibracores, resulting in a lithostratigraphic framework for the two shoals. The magnetometer data provided an array of magnetic anomalies that defined the oil and gas

infrastructure in the study area as well as other anomalies that identify randomly distributed metallic objects away from oil and gas pipelines and production facilities. Because of the importance of the magnetometer anomalies in defining both the oil and gas infrastructure as well as other metallic objects, a table of anomalies and their mapped spatial distributions are presented in Appendix 50. These and all other project datasets are provided in digital format on a DVD (Appendix 51).

Using both the subbottom data to determine sediment body geometry and the vibracores to define sand facies it was possible to calculate sand volumes in Tiger and Trinity Shoal Complex. In addition, the quality of the sand was determined by analyzing subsamples of the sand facies in each vibracore. Most sand samples fell in the fine sand category. The grain size analysis results for each sample analyzed are included in Appendices 4 to 49 with other data collected on each vibracore. Using the Petrel^{TM} software the total sand volume in Tiger Shoal was calculated at 58.6 x 106 yd^3 (44.8 x 10^6 m^3), while the total sand volume in the much larger Trinity Shoal was 893.2 x 10^6 yd^3 (686.7 x 106 m^3), Table 3. However, because of the oil and gas infrastructure that crosses each shoal not all of the sand is available for potential extraction. Table 4 lists sand volumes in five areas defined by oil and gas infrastructure and free of pipelines and production platforms. These areas were calculated using a 1000 ft (305 m) buffer zone from pipelines as mandated by state and federal regulations regarding sand extraction. Figure 16 and the larger map of Appendix 50 illustrate the distribution of magnetic anomalies and the recommended areas of potential sand extraction defined by the network of pipelines and production platforms in the area of the shoals.

It is important to note that the estimates of total sand in the Tiger and Trinity Shoals as calculated from the datasets collected in this project are less than half of the total sand volume published as a result of the 1980s study by Penland et al., 1990 (Table 3). The total sand volume estimates from Penland et al. (1990) for Tiger and Trinity Shoals are 2.6 billion yd^3 (2 billion m^3) as compared to 933.3 million yd^3 (731.6 million m^3) as calculated from the recent investigation described in this report. Even though our estimate is considerably less than the earlier one, there is still an enormous volume of sand stored in these shoals. Not all of this sand, however, can be considered a resource for coastal restoration. The rather extensive oil and gas infrastructure in the shoal complex area, as defined by magnetometer anomalies (Figure 16), causes the sand bodies to be partitioned with regard to sand extraction. Five areas are defined by this infrastructure. Table 4 provides the sand volumes available for extraction. These estimates range from 19.6 x 10^6 yd^3 (15.0 x 10^6 m) in an infrastructure-limited part of Tiger Shoal to 158 x 10^6 yd^3 (121.1 x 10^6 m^3) in the largest of four sectors defined for Trinity Shoal. These sectors are primarily defined by pipelines crossing the shoal. Magnetic anomalies clearly define this infrastructure. There are, however, a few magnetic anomalies scattered within the five polygons identified for potential future sand extraction. Although these anomalies would need to be examined in detail before these polygons could be cleared for sand dredging, their gamma deflections (strength of the anomaly) are generally small and the anomalies are isolated and do not align into trends. They are therefore interpreted as scattered small-scale metallic debris, probably from oil and gas activity in the area.

In summary, we confirm with this study that the Tiger and Trinity Shoal Complex represents a large combined deposit of sand that could be extremely useful to the State of

Louisiana for restoration projects along the central coast of our state. Although there is considerable oil and gas activity in the area, there are sectors of both shoals, particularly Trinity Shoal, that could be mined for sand. If no new oil and gas infrastructure is developed, the areas defined by this study contain sand that can be extracted for state needs.

Finally, all datasets collected as part of this investigation will be submitted to OCPR in digital format for input into the Louisiana Sand Resources Database (LASARD).

REFERENCES

Allen, Y.C., C.A. Wilson, H.H. Roberts, and J. Supan, 2005, High resolution mapping and classification of oyster habitats in nearshore Louisiana using sidescan sonar: Estuaries, v. 28, p. 435-446.

Autin, W.J., S.F. Burns, B.J. Miller, R.T. Saucier, and J.I. Snead, 1991, Quaternary geology of the Lower Mississippi Valley, *in* Morrison, R.B. (ed.), Quaternary nonglacial geology: Conterminous U.S.: Geological Society of America, Boulder, CO, p. 547-582.

Barras, J.A., D. Beville, S. Britsch, S. Hartley, J. Hawes, P. Johnston, Q. Kemp, A. Kinler, J. Martucci, D. Porthouse, K. Reed, S. Roy, S. Sapkota, and J. Suhayda, 2003, Historical and Projected Coastal Louisiana Land Changes: 1978–2050. USGS Open File Report 03-334.

Barras, J.A., 2006, Land Area Change in Coastal Louisiana after the 2005 Hurricanes – A Series of Three Maps: U. S. Geological Survey Open-File Report 06-1274.

Barras, J.A., J.C. Bernier, and R.A. Morton, 2008, Land change in coastal Louisiana: a multidecadal perspective (From 1956 to 2006): U.S. Geological Survey Scientific Investigations Map 3019, Scale 1:250,000.

Barras, J.A. J.C. Bernier, and R.A. Morton, 2008, Land area change in coastal Louisiana—a multidecadal perspective (from 1956 to 2006): U.S. Geological Survey Scientific Investigations Map 3019, scale 1:250,000, 14p. Pamphlet, http://pubs.usgs.gov/sim/3019/.

Blum, M.D. and H.H. Roberts, 2009, Drowning of the Mississippi Delta due to insufficient sediment supply and global sea-level rise. Nature Geoscience, v. 2, p. 488–491.

Britsch, L.D. and J.B. Dunbar, 1993, Land-loss rates—Louisiana coastal plain. Journal of Coastal Research, v. 9, p. 324–338.

Coleman, J.M. and S.M. Gagliano, 1964, Cyclic sedimentation in the Mississippi River Delta Plain: Transactions Gulf Coast Association of Geological Societies, v. 14, p. 67-80.

Dahl, T.E., 2000, Status and Trends of Wetlands in the Conterminous United States 1986 to 1997. Washington D.C.: U.S. Department of the Interior, Fish and Wildlife Service.

Field, D.W., A. Reyer, P. Genovese, and B. Shearer, 1991, Coastal Wetlands of the United States—An Accounting of a Valuable National Resource. Rockville, Maryland: Strategic Assessment Branch, Ocean Assessments Division, Office of Oceanography and Marine Assessment, National Ocean Service, National Oceanic and Atmospheric Administration.

Finkl, C.W. and S.M. Khalil, 2005, Offshore exploration for sand sources: general guidelines and procedural strategies along deltaic coasts. In: Finkl, C.W. and Khalil, S.M. (eds.),

Savings America's Wetland: Strategies for Restoration of Louisiana's Coastal Wetlands and Barrier Islands. Journal of Coastal Research, Special Issue No. 44, pp. 203–233.

Finkl, C.W. S.M. Khalil, J. Andrews, S. Keehn, and L. Benedet, 2006, Fluvial sand sources for barrier island restoration in Louisiana: Geotechnical investigations in the Mississippi River. Journal of Coastal Research, v. 22, p. 773–787.

Fisk, H.N., 1944, Geological investigation of the alluvial valley of the Lower Mississippi River: U.S. Army Corp of Engineers, Mississippi River Commission, Vicksburg, Mississippi, 78 p.

Fisk, H.N. and E. McFarlan, Jr., 1955, Late Quaternary deltaic deposits of the Mississippi River: Geological Society of America Special Paper, no. 62, p. 279-302.

Fisk, H.N. and B. McClelland, 1959. Geology of the continental shelf off Louisiana: Its influence on offshore foundation design: Geological Society of America Bulletin, v. 70, p. 1369-1394.

Folk, R. L. and W. Ward, 1957, Brazos River Bar: A Study in the Significance of Grain Size Parameters: Journal of Sedimentary Petrology, v. 27, p. 3-26.

Folk, R. L., 1974, Petrology of Sedimentary Rocks: Austin, Texas, Hemphill Publishing, 182 p.

Frazier, D.E., 1967, Recent deltaic deposits of the Mississippi River: Their development and chronology: Transactions Gulf Coast Association of Geological Societies, v. 17, p. 287-315.

Georgiou, I.Y, D.M. FitzGerald, and G.W. Stone, 2005, The impact of physical processes along the Louisiana coast: Journal of Coastal Research, v. 44, p. 72-89.

Guidroz, W.S., G.W. Stone, and D. Dartez, 2005, Hurricane Rita, 2005: Assessment of a storm-induced geological event along the southwestern Louisiana coast and adjacent interior marshland: Gulf Coast Association of Geological Societies Transactions, v. 56, p. 229-239.

Jackson, D. R. and M. D. Richardson, 2007, High-frequency seafloor acoustics: New York, Springer Science, 616 p.

Keim, B.D., R.A. Muller, and G.W. Stone, 2007, Spatiotemporal patterns and return periods of tropical storm and hurricane strikes from Texas to Maine. Journal of Climate, v. 20, p. 3498–3508.

Khalil, S.M. 2004, General Guidelines: Exploration for Offshore Sand Sources, Version-IV: Coastal Engineering Division. OCRM, Louisiana Department of Natural Resources, Baton Rouge, LA.

Khalil, S.M., 2008, General Guidelines: Exploration of offshore sand sources. Baton Rouge, Louisiana Department of Natural Resources, OCRM, Coastal Engineering Division, Version V.

Kolb, C.R. and Van Lopik, J.R., 1958, Geology of the Mississippi River Deltaic Plain, southeastern Louisiana: U.S. Army Engineer Waterways Experiment Station, Vicksburg, Mississippi, Technical Report 2, 482 p.

Liner, C.L., 2004, Elements of 3D Seismology 2nd Edition: Tulsa, Oklahoma, PennWell, 608 p.

Peltier, W.R. and R.G. Fairbanks, 2006, Global glacial ice volume and Last Glacial Maximum duration from an extended Barbados sea level record: Quaternary Science Reviews, v. 25, p. 3322-3337.

Penland, S. and R. Boyd, 1981, Shoreline changes on the Louisiana barrier coast: IEEE Oceans, v. 81, p. 209-219.

Penland, S., J.R. Suter, and R. Boyd, 1985, Barrier island arcs along abandoned Mississippi River deltas: Marine Geology, v. 63, p. 197-233.

Penland, S., R. Boyd, and J.R. Suter, 1988, Transgressive depositional systems of the Mississippi Delta Plain: A model for barrier shoreline and shelf sand development: Journal of Sedimentary Petrology, v. 58, p. 932-949.

Penland, S., R. Boyd, and J.R. Suter, 1988, Transgressive depositional systems of the Mississippi River delta plain. Journal of Sedimentary Petrology, v. 58, p. 932–949.

Penland, S., R. Boyd, and J. R. Suter, 1988, Transgressive Depositional Systems of the Mississippi Delta Plain: A Model for Barrier Shoreline and Shelf Sand Development: Journal of Sedimentary Petrology, v. 58, p. 932-949.

Penland, S., J.R. Suter, R.A. McBride, S.J. Williams, J.L. Kindinger, and R. Boyd, 1989, Holocene sand shoals offshore of the Mississippi River delta plain. Gulf Coast Association Geological Societies Transactions, v. 39, p. 471–480.

Penland, S., D.L. Pope, R.A. McBride, J.R. Suter, and C.G. Groat, 1990, Assessment of sand resources in the Trinity Shoal area, Louisiana continental shelf: Louisiana Geological Survey, Cooperative Agreement Submitted to U.S. Minerals Management Service No. 14-12-0001-30387, 46 p.

Pope, D. L., S. Penland, J. R. Suter, and R. McBride, 1991, Holocene Geologic Framework of the Trinity Shoal Region, Louisiana Continental Shelf: GCSSEPM Foundation 12th Annual Research Conference Proceedings, p. 191-201.

Roberts, H.H., 1997, Dynamic changes of the Holocene Mississippi River Delta Plain: The delta cycle: Journal of Coastal Research, v. 13, p. 605-627.

Roberts, H.H., 1997, Dynamic changes of the Holocene Mississippi River delta plain—the delta cycle. Journal of Coastal Research, v.13, p. 605–627.

Roberts, H.H., C.A. Wilson, J. Supan, and W. Winans, 1999, New technology for characterizing Louisiana's shallow coastal water bottoms and predicting future changes: Transactions Gulf Coast Association of Geological Societies, v. 49, p. 451-460.

Roberts, H.H., C. Wilson, and J. Supan, 2000, Acoustic surveying of ultra-shallow water bottoms (< 2m) for both engineering and environmental applications: Proceedings Offshore Technology Conference, 1-4 May 2000, Houston, Texas, OTC Paper 12108, p. 1-10.

Roberts, H. H., N. D. Walker, and A. Sheremet, 2005, Effects of Cold Fronts on Bayhead Delta Development: Atchafalaya Bay, Louisiana, U. S. A.: In D. M. Fitzgerald and J. Knight (eds.), High Resolution Morphodynamics and Sedimentary Evolution of Estuaries: Kulmer Academic Publishers, Dordrecht, The Netherlands, p. 269-298.

Saucier, R.T., 1994, Geomorphology and Quaternary geologic history of the Lower Mississippi Valley: U.S. Army Engineer Waterways Experiment Station, Vicksburg, Mississippi, 364 p.

Scruton, P.C., 1960, Delta building and the deltaic sequence, *in* Trask, P.D. (ed.), Recent Sediments, Northwest Gulf of Mexico: American Association of Petroleum Geologists, Tulsa, Oklahoma, p. 82-102.

Stone, G.W., X. Zhang, and A. Sheremet, 2005, The role of barrier island, muddy shelf, and reefs in mitigating the wave field along coastal Louisiana: Journal of Coastal Research, v. 44, p. 40-55.

Suter, J.R. S. Penland, and K.E. Ramsey, 1991, Nearshore Sand Resources of the Mississippi River Delta Plain: Marsh Island to Sandy Point. Baton Rouge, Louisiana: Louisiana Geological Survey, Coastal Geology Technical Report No. 8, 130p

Schultheiss, P.J. and S.D. McPhail, 1989, An automated P-wave logger for recording fine-scale compressional wave velocity structures in sediments: Proceedings Ocean Drilling Program, Scientific Results, v. 108, p. 407-413.

Schultheiss, P.J. and P.P.E. Weaver, 1992, Multi-sensor core logging for science and industry: In: Proceedings Ocean 92, Mastering the Oceans Through Technology v. 2, p. 608-613.

Walker, N. D. and A. D. Hammack, 2000, Impacts of Winter Storms on Circulation and Sediment Transport: Atchafalaya-Vermillion Bay Region, Louisiana, U. S. A.: Journal Coastal Research, v. 16, p. 996-1010.

ACKNOWLEDGMENTS

This investigation was funded by the US Department of the Interior Minerals Management Service, MMS (now the Bureau of Ocean Energy Management, Regulation and Enforcement, BOEMRE) to the Louisiana Department of Natural Resources, DNR (now the Louisiana Office of Coastal Protection and Restoration, OCPR) through Cooperative Agreement No. M07AC 12517. The Louisiana Department of Natural Resources (OCPR) contracted Coastal Studies Institute (CSI) at Louisiana State University (LSU) through Interagency Agreement No. 2512-07-12 to conduct a geological investigation to evaluate the sand resources of the Tiger-Trinity Shoals Complex. We acknowledge the help and guidance of Mr. Roger Amato of BOEMRE, the project officer who was kind enough to support the project with both administrative and technical help. We gratefully acknowledge the excellent technical support in both the field and laboratory by the Coastal Studies Institute Field Support Group (Walker Winans, Floyd DeMers, Chris Cleaver, Darren Depew, and Charlie Sibley). This project could not have been efficiently executed without the logistical support of one of our colleagues, Eddie Weeks, and his parents, Ned and Barbara Weeks, who allowed us to use their camp at Cypremort Point as a base of operations. Without access to the Weeks' camp, our productivity on this project would have been severely diminished. For their support of our project we sincerely thank them. We also want to thank April Hawkins for help with report preparation and Mary Lee Eggart for her professional artistic assistance with illustrations.

We would like to thank Schlumberger and the Department of Geology and Geophysics at Louisiana State University for access to Petrel™ software, which was provided through a grant from Schlumberger. We are also grateful for access to the Harrison Family Subsurface Laboratory within the Department of Geology and Geophysics at Louisiana State University where we used Seismic Unix, which was essential to the initial stages of processing our seismic data. We are grateful to Dr. Felix Jose and Dr. Baozhu Liu for their assistance with ArcGIS.